Iron and copper complexation in Macaronesian coastal waters

V. Arnone, D. González-Santana, M. González-Dávila [*], A.G. González [*], J.M. Santana-Casiano

Instituto de Oceanografía y Cambio Global, IOCAG, Universidad de Las Palmas de Gran Canaria, ULPGC, 35017 Las Palmas de Gran Canaria, Spain

ARTICLE INFO

ABSTRACT

Dissolved iron (dFe) and copper (dCu), the concentration and the conditional stability constants of organic binding ligands (L_{Fe}, L_{Cu}, log K^{cond}_{Fe3+L} and log K^{cond}_{Cu2+L}) were studied in the surface coastal waters of the Macaronesia region (Cape Verde, Canary Islands, and Madeira) using competitive ligand exchange-adsorptive cathodic stripping voltammetry (CLE-ACSV). Two oceanic stations were also studied: the Cape Verde Ocean Observatory (CVOO) and the European Station for Time Series in the Ocean in the Canary Islands (ESTOC). Dissolved Fe varied from 0.46 to 1.32 nM and L_{Fe} concentrations were between 0.56 and 2.96 nM. More than 98% of the total dFe was complexed with conditional stability constants (log K^{cond}_{Fe3+L}) between 20.77 and 21.90 (L_2-type ligands). Dissolved Cu concentrations ranged between 0.07 and 4.03 nM and the amount of L_{Cu} varied between 0.54 and 2.59 nM, with more than 99% of dCu organically complexed. The conditional stability constant (log K^{cond}_{Cu2+L}) showed values between 13.40 and 14.42 (L_1-type).

Due to biological activity and water mixing induced by the wind around the islands, dissolved metals and ligand concentrations were greater at the coastal stations than in oceanic water. Variations were observed between the eastern and western parts of Fogo, Tenerife and Gran Canaria. On the east coasts, the increase in dissolved metals and ligand concentrations were related to wind-induced water mixing. The results of this study will contribute to the knowledge about the impact of coastal areas on the Fe and Cu biogeochemical cycles.

1. Introduction

Iron (Fe) and copper (Cu) are essential trace metals for marine microorganisms, as they are involved in many metabolic processes. Iron is essential for photosynthesis, respiration processes (Morel and Price, 2003; Raven et al., 1999) and nitrogen fixation (Mills et al., 2005; Moore et al., 2001) and is used in superoxide dismutase (SOD) (Wolfe-Simon et al., 2005), as well as in the nitrate and nitrite reductase processes (Sunda, 1989; Twining and Baines, 2013). Copper is an important constituent in different enzyme systems related to a variety of processes including photosynthetic and mitochondrial electron transport (Sunda, 1989). However, high concentrations of free cupric ion (Cu^{2+}) are toxic to certain marine organisms and can inhibit phytoplankton growth (Brand et al., 1986; Morel et al., 1978; Sunda and Lewis, 1978). Copper is also a cofactor involved in the Fe transport reaction (Peers et al., 2005).

Iron and Cu are similar in some biogeochemical aspects. Both trace metals are present in seawater in two different oxidation states, and the oxidized species are the most thermodynamically stable in oxic waters (González-Dávila et al., 2009; Santana-Casiano et al., 2005). The formation of organic complexes with dFe and dCu dominates the speciation of both metals (>99%). This may increase Fe solubility, stabilizing it against the oxy-hydroxide formation and precipitation (Liu and Millero, 2002; Rue and Bruland, 1995) and thus increasing its residence time and bioavailability (Buck et al., 2007; Hutchins et al., 1999; Kuma et al., 1996; Maldonado and Price, 1999). Different models show that phytoplankton can use complexed Fe to obtain free metal which is available for biological uptake (Morel et al., 2008). In the case of Cu, organic complexation reduces the scavenging and promotes the decrease of free Cu^{2+}, controlling its bioavailability and toxicity. A fraction of the Cu-ligand complexes may also contribute to Cu uptake (Annett et al., 2008; Semeniuk et al., 2015, 2009). The Fe and Cu-binding ligands (L_{Fe} and L_{Cu}) present different sources such as: rupture of cells after grazing (Sato et al., 2007), viral lysis (Poorvin et al., 2011), transformation of organic matter (Gerringa et al., 2006), phytoplankton exudates (Rico et al., 2013; Santana-Casiano et al., 2014) and sediments (Gerringa et al., 2008). The L_{Fe} and L_{Cu} are classified according to the value of the conditional stability constants (log K^{cond}_{Fe3+L} and log K^{cond}_{Cu2+L}). These ligands can be considered to be strong (L_1) or weak (L_2), where log K^{cond}_{Fe3+L} = 22 divides L_1 and L_2-type of Fe-binding

---

ligands (Gledhill and Buck, 2012). For Cu, the value which splits ligands type corresponds to log $K^{cond}_{Cu2+L} = 13$ (Bruland et al., 2000; Buck and Bruland, 2005).

In the Atlantic Ocean surface waters, dFe concentrations range between 0.1 and 0.8 nM (Boye et al., 2006; Rijkenberg et al., 2008) with variations between different areas of the ocean depending on Fe sources, mesoscale processes and primary production. In the North Atlantic oceanic region, between 71% and 87% of surface dFe comes from the aeolian deposition of Saharan dust (Conway and John, 2014). However, Fe solubilization from aeolian input is low (~1.7%, Baker et al., 2006) and previous work has shown the concentration of dFe increase by 0.05–0.10 nM after a dust event (Rijkenberg et al., 2012, 2008). Surface dCu concentrations vary between 0.7 and 5.9 nM (Buckley and van den Berg, 1986; Saager et al., 1997). The presence of Saharan dust does not influence the concentration of dCu in the North Atlantic surface waters (Jacquot and Moffett, 2015).

The Fe speciation in the oceanic and upwelling region of the Northeast Atlantic Ocean has been previously studied (Boye et al., 2006, 2003; Buck et al., 2015; Gerringa et al., 2006; Gledhill and van den Berg, 1994; Rijkenberg et al., 2012, 2008; Thuróczy et al., 2010). These investigations showed variable values of log K^{cond}_{Fe3+L} (18.8–22.85) and L_{Fe} concentration ranging from 0.82 to 4.08 nM. However, Cu speciation in the open ocean of the Atlantic Ocean has been poorly studied. Research has mainly focused on polar waters (Buck et al., 2010; Bundy et al., 2013; Heller and Croot, 2015), Pacific oceanic waters (Coale and Bruland, 1990; Ruacho et al., 2020; Whitby et al., 2018) and coastal environments influenced by rivers (Abualhaija et al., 2015; Gledhill et al., 2015). Few speciation studies have been conducted in the Atlantic Ocean (Buckley and van den Berg, 1986; Jacquot and Moffett, 2015; Moffett et al., 1990). For the North Atlantic Ocean, a log K^{cond}_{Cu2+L} of 13.6 ± 0.5 and a L_{Cu} of 2.6 ± 0.8 nM have been reported (Jacquot and Moffett, 2015).

The surrounding waters of oceanic islands are characterized by very complex and dynamic environments where a high concentration of phytoplankton biomass is typically observed (Blain et al., 2007, 2001). Various studies (Blain et al., 2008, 2007, 2001; Gerringa et al., 2008) in the vicinity of the Kerguelen Islands (Southern Ocean) have shown that different processes act as a source of micronutrients, particulate Fe (Bowie et al., 2015) and dFe-ligands (Gerringa et al., 2008; Monteiro and Orren, 1985) and thus promote phytoplankton growth. Different dFe sources can be found, such as the horizontal advection, the vertical mixing, the isopycnal mixing, the atmospheric dust deposition and the consequent dissolution from lithogenic particulate Fe (Blain et al., 2008). However, regeneration from biogenic material and the input from the sediments are the most important sources of dFe above the plateau (Blain et al., 2008; Elrod et al., 2004). Due to the importance of Fe supply in the phytoplankton production and CO_2 sequestration, numerous studies have been carried out in islands of the Southern Ocean (Blain et al., 2008, 2007, 2001; Gerringa et al., 2008; Planquette et al., 2007; Robinson et al., 2016) and around the Pacific Ocean (Gordon et al., 1998; Kondo et al., 2007; Raapoto et al., 2019). However, the contribution of micronutrients and organic ligands from islands in other oceanic regions is still poorly understood understudied.

The Macaronesia region in the Northeast Atlantic Ocean is a large area from the Cape Verde archipelago to the Azores islands, dominated by many processes such as mesoscale eddies, filaments and coastal upwelling (Caldeira et al., 2002; Pelegrí et al., 2017; Sangrà et al., 2009). The complex hydrodynamic affects the distribution of metals and ligands in both oceanic and nearshore areas. Across the region, temperature increases and precipitation decreases towards the Equator (Mehlmann et al., 2020). The interaction between the orography and trade winds controls the weather of each island and the region between them. There is no riverine input to the coastal waters. However, when it rains, there is non-continuous input through runoff and ravines subject to the rainfall regime, which is variable and very scarce on some islands. The chemical speciation of Fe could be influenced by these sporadic

contributions and also by the great input of atmospheric dust deposition from the Sahara desert and Sahel region (Duce and Tindale, 1991; Gelado-Caballero et al., 2012; López-García et al., 2021). Another factor that could influence Fe and Cu speciation are the anthropogenic sources. In each archipelago there are power plants and desalination plants, which together with wastewater can alter the chemical composition of coastal waters.

During early spring 2019 dFe and dCu speciation were measured in coastal surface waters in three different archipelagos in the Macaronesia region (Cape Verde, Canary Islands and Madeira). The concentration of dFe and dCu, and the concentration and characteristics of Fe and Cu-binding ligands were measured by Competitive Ligand Exchange-Adsorptive Cathodic Stripping Voltammetry (CLE-ACSV). The results from this research will show the first dataset on dFe and dCu speciation in the coastal waters of the Macaronesia Islands, increasing our knowledge of the Fe and Cu biogeochemical cycles.

2. Materials and methods

2.1. Sampling strategy

The POS533 cruise took place during early spring (from February 29 to March 19, 2019) on board the *R/V Poseidon* in the eastern Atlantic Ocean, along the Macaronesian archipelagos (Cape Verde, Canary Islands and Madeira). Seawater samples were taken in coastal and oceanic stations by following a path from south to north (Fig. 1), starting from Cape Verde and finishing in Madeira.

The exact location of each station is shown in Fig. 2. In the Cape Verde region (Fig. 2a), samples were taken in coastal waters near the islands of Santo Antão (St. 1), São Nicolau (St. 4), Fogo (St. 6), Santiago (St. 9), Maio (St. 11), Boa Vista (St. 13), Sal (St. 14) and São Vicente (St. 16). One oceanic station (St. 17) was sampled at the Cape Verde Ocean Observatory (CVOO) located north of the archipelago.

In the Canary Islands (Fig. 2b), the coasts of El Hierro (St. 21), La Gomera (St. 25), Tenerife (St. 31, 32 and 34) and Gran Canaria (St. 39, 40 and 42) were sampled. One station was located between the islands of El Hierro and La Gomera (St. 23) and one between Tenerife and Gran Canaria (St. 37). An oceanic station was positioned at the European Station for Time Series in the Ocean in the Canary Islands (ESTOC), located north of the archipelago.

Another set of coastal samples were obtained in the Salvages Islands (St. 45, Fig. 2b), Desertas Islands (St. 52, Fig. 2c), in the channel between Desertas Islands and Madeira (St. 54, Fig. 2c) and in the south of Madeira (St. 63, Fig. 2c).

2.2. Sampling

Seawater samples for dFe, dCu and ligand (L_{Fe} and L_{Cu}) measurements were collected at 20 m depth at coastal and oceanic stations (Fig. 2) using a trace metal clean PFA Teflon diaphragm pump connected to PFA Teflon tubing, and filtered online (0.2 μm Acropack Supor®, 6.4 mm MNPT/ 6.4–12.7 mm). During sampling, the acid-cleaned low-density polyethylene (LDPE) bottles were triple rinsed with the seawater sample before filling the bottle, double bagged and kept in the dark at −20 °C. For each metal, 250 mL of seawater was sampled in separate bottles. The procedure followed the protocol described by Buck et al. (2012) and Cutter et al. (2010).

For hydrographic information, temperature and salinity data were recorded from a CTD coupled to the rosette. The pH (total scale) was measured using the UV–Vis spectrophotometric technique (Clayton and Byrne, 1993) with m-cresol purple as an indicator with a standard deviation of ± 0.002 (González-Dávila et al., 2003). Dissolved oxygen was measured on board by using the Winkler Titration (Grasshoff et al., 1999). Nutrients used for the statistical analysis, were collected in 14 mL polyethylene tubes to determine the content of nitrate and nitrite ($NO_3^- + NO_2^-$), phosphate (PO_4^{3-}) and silicates ($Si(OH)_4$) performing the
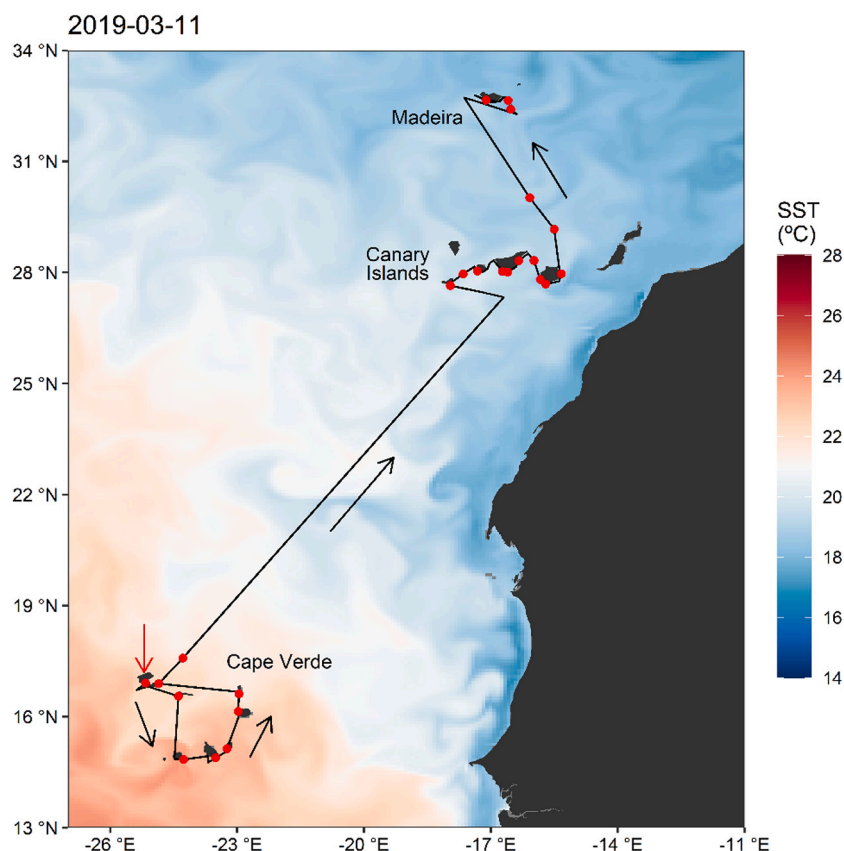
Fig. 1. Representation of POS533 cruise track (black line) over a sea surface temperature image (COPERNICUS product) of March 11 (2019). The cruise took place between February 29 and March 19 (2019). The sampling started in Cape Verde (St. 1, red arrow) and ended in Madeira. The station locations are marked by red dots.

spectrophotometric analysis (Grasshoff et al., 1999) with a QuAAtro auto-analyser (SEAL Analytical, UK).

2.3. Instrumentation and reagents

Iron and Cu stock solutions were prepared weekly from standard solutions for atomic absorption spectrometry (Fluka), diluted with MQ-water and acidified with 100 μL ultrapure 12.8 M HCl.

A 1.0 M stock buffer of EPPS (N-(2-hydroxyethyl)piperazine-N′;2-propanesulfonic acid; *Sigma-Aldrich*) was prepared in 1.0 M ultrapure NH_4OH (VWR) at pH 8.2. Possibly remaining metals were removed from the buffer solution by adding 100 μM of MnO_2, stirred overnight and filtrated through an acid-clean 0.45 μm filter (Campos and van den Berg, 1994).

For the Fe analysis, a 0.01 M stock solution of TAC (2-(2-thiazoly-lazo)-p-cresol; Sigma-Aldrich) was prepared in methanol (Sigma-Aldrich). For Cu analysis, a 0.01 M solution of SA (salicylaldoxime; Sigma-Aldrich) was prepared in 0.1 M ultrapure HCl. All stock solutions were kept in the fridge when they were not in use (darkness and 8 °C).

The dFe and dCu concentrations and the speciation were measured by CLE-ACSV on an Epsilon voltammeter (Basi, Inc) connected with a hanging mercury drop electrode (CGME, Basi, Inc). The reference electrode was Ag/AgCl with a salt bridge filled with 3 M KCl, with a platinum auxiliary electrode. The solution was mixed during the deposition time and purged by bubbling with high purity nitrogen. The first two drops of the mercury drop electrode were always discarded, and the third mercury drop was used. Voltammetric conditioned cells (PTFE) were always used.

2.4. dFe and dCu concentration

Dissolved Fe concentrations were determined by CLE-ACSV with ligand competition against TAC (Croot and Johansson, 2000) using the method of standard additions. An aliquot (10 mL) of the seawater sample was UV-irradiated for 4 h in a quartz tube, then 20 μL of TAC and 100 μL of 1 M EPPS were added. The differential pulse stripping voltammetry (DPSV) conditions for Fe measurements were: deposition potential at −410 mV for 120 s, quiet time for 5 s, initial potential at −410 mV and final potential at −600 mV. The step was 2 mV, pulse width of 10 ms, pulse period of 100 ms and pulse amplitude of 50 mV.

The dCu concentration was determined by using SA as a competitive ligand (Campos and van den Berg, 1994) with the standard addition method. The samples were prepared with 20 μL of 0.01 M SA and 100 μL of 1 M EPPS. The DPSV conditions for Cu measurements were: deposition potential at −50 mV for 100 s, quiet time for 10 s, initial potential at −150 mV and final potential at −600 mV. The step was 4 mV, pulse width of 50 ms, pulse period of 200 ms and pulse amplitude of 50 mV.

2.5. dFe and dCu speciation

For the determination of dFe complexation, 10 mL samples were pipetted into 15 Teflon bottles, 100 μL of EPPS (final concentration 10^{-2} M) and different concentrations of Fe were added (from 0 to 10 nM). After a 1 h equilibration period, 10 μL of TAC (final concentration 10 μM) was added and left to equilibrate overnight (Croot and Johansson, 2000). The titration series were measured in a Teflon cell, with two +0 Fe additions and more than 10 titration points (Garnier et al., 2004; Gledhill and Buck, 2012).

The procedure used to determine the dCu speciation was the same but using 10 μL of SA (final concentration 10 μM) (Campos and van den
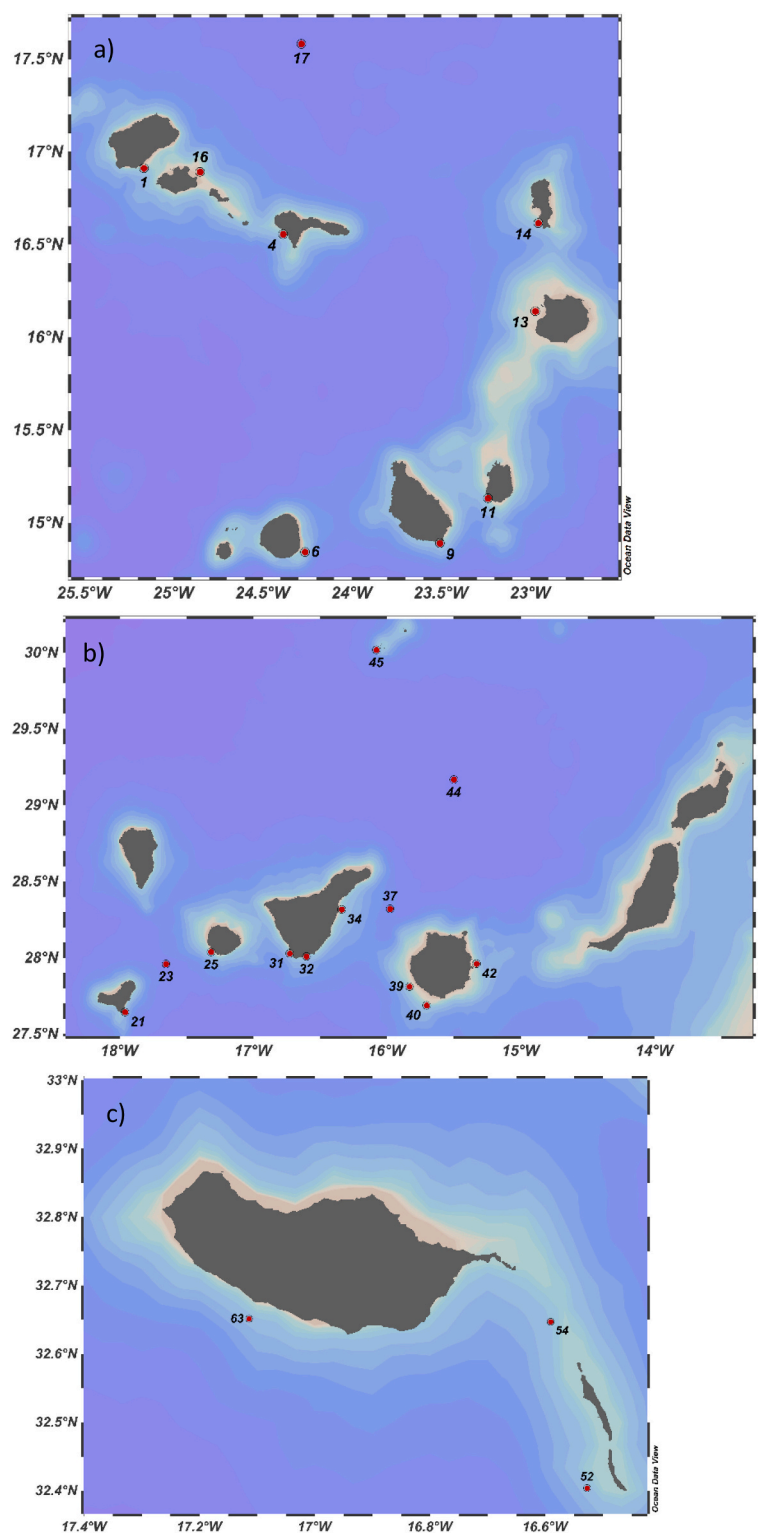
Fig. 2. Sampling locations along the cruise POS533 in the three regions Madeira (a), Canary Islands (b) and Cape Verde (c).

Berg, 1994). Under the buffer conditions for those determinations, the inorganic metal side reaction coefficients are $\alpha_{Cu'} = 32$ (Pižeta et al., 2015) and $\alpha_{Fe'} = 10^{10}$ (Hudson et al., 1992), respectively, controlled by the pH, temperature and salinity of the sample.

The dCu and dFe speciation in seawater, the dCu and dFe-binding ligands (L_{Cu} and L_{Fe}), and the conditional stability constants (K^{cond}_{CuLi} and K^{cond}_{FeLi}) were computed using the ProMCC software (Omanović et al., 2015). One ligand class model fitted the experimental values. All

the stability constants determined and indicated in the paper are conditional to the experimental seawater conditions for the samples. The dFe and dCu speciation and concentration data are accessible in the database PANGAEA (Santana-Casiano and Quack, 2021).

2.6. Theory

Considering the dissolved phase (<0.2 μm), the dissolved

concentration of a metal (dM), both for Fe and Cu, in a natural seawater sample can be defined as:

$$dM = [M'] + [ML] \tag{1}$$

Where [M] represents the labile metal concentration, defined as the sum of all inorganic species including M^{n+}. [ML] is the concentration of metal complexed with organic ligands (L). The reaction between M′ and the labile natural binding ligands (L) can be expressed as:

$$M' + L' \rightleftharpoons ML \tag{2}$$

The conditional stability constant of the formed complex (K^{cond}_{ML}) describes the strength of a binding ligand and is calculated from:

$$K^{cond}_{M'L} = \frac{[ML]}{[M'][L']} \tag{3}$$

[M] is related with $[M^{n+}]$ by the inorganic side reaction coefficient (α_M):

$$[M'] = \alpha_{M'} \bullet [M^{n+}] \tag{4}$$

In terms of ionic metal (M^{n+}), the conditional stability constant can be calculated from:

$$K^{cond}_{M^{n+}L} = \alpha_{M'} \bullet K^{cond}_{M'L} \tag{6}$$

The reactivity of the metal, M, with the natural binding ligands (f_{ML}) describes the complexation capacity of dissolved ligands to be bound with M (Gledhill and Gerringa, 2017). This coefficient can be estimated in respect to M′ and M^{n+} as expressed below:

$$f_{M'L} = K^{cond}_{M'L} \bullet [L_M] \tag{7}$$

$$f_{M+L} = K^{cond}_{M^{n+}L} \bullet [L_M] \tag{8}$$

The excess ligand (eL_M) represents the concentration of free M-binding sites (Thuróczy et al., 2011) and indicates the saturation state of ligands. The eL_M was defined as:

$$[eL_M] = [L_M] - [dM] \tag{9}$$

The L_M/dM ratio indicates the saturation state of the natural ligand and values close to 1 designate that most of the ligands are bound with the metal. For Fe, ratios near 1 indicate a high potential for metal precipitation, while higher values denote a great potential for metal solubilization (Thuróczy et al., 2011).

To determine the speciation of M through CLE-ACSV, it is necessary to add a well-characterized ligand (AL) that reacts with M and competes with ML to form a new complex (MAL). The MAL is an electroactive complex that can be adsorbed onto the mercury drop and undergo a reduction. Further details on the determination of the speciation of Fe by using TAC can be found in Croot and Johansson (2000). For the speciation of Cu, further information can be found in Campos and van den Berg (1994).

The "detection window" or analytical window determines the concentration of the ligands and the conditional stability constant that can be estimated with the titration. The side reaction coefficient of the MAL complex (α_{MAL}) represents the centre of the detection window (D), which is defined as the product of the AL concentration (AL) and the conditional stability constant for the MAL complex. The higher the α_{MAL} value, the greater its ability to form complexes and compete with other ligands. This allows stronger complexes to be detected (with higher K^{cond}_{ML} or K^{cond}_{Mn+L} values) but results in a lower concentration of ligands (Buck et al., 2012; Campos and van den Berg, 1994). For Fe, the analytical window is defined as:

$$\alpha_{Fe(TAC)_2} = \beta^{cond}_{Fe(TAC)_2} \bullet [TAC]^2 = D \tag{10}$$

For a TAC concentration of 10 μM, $\beta^{cond}_{Fe(TAC)2}$ takes a value of $10^{12.4}$ (Croot and Johansson, 2000) then $\alpha_{Fe(TAC)2} = 251$. For Cu, the detection window is given by:

$$\alpha_{CuSA} = K^{cond}_{CuSA} \bullet [SA] + \beta^{cond}_{Cu(SA)_2} \bullet [SA]^2 = D \tag{11}$$

Where both stability constants were calculated as a function of salinity, S (Campos and van den Berg, 1994):

$$log K^{cond}_{CuSA} = 10.12 - 0.37 \bullet logS \tag{12}$$

$$log \beta^{cond}_{Cu(SA)_2} = 15.78 - 0.53 \bullet logS \tag{13}$$

Considering a 10 μM concentration of SA and sample salinity, α_{CuSA} presented values between 5.09 and 5.10.

2.7. Statistical analysis

The data were analysed by Principal Components Analysis (PCA) using the PAST software. The PCA analysis (Fig. 3) was applied, considering the following variables: temperature, salinity, fluorescence, turbulence, dFe, dCu, $NO_3^- + NO_2^-$, PO_4^{3-} and $Si(OH)_4$. Since the variables have different units, the programme's tool has been used to normalise the data by considering their standard deviation.
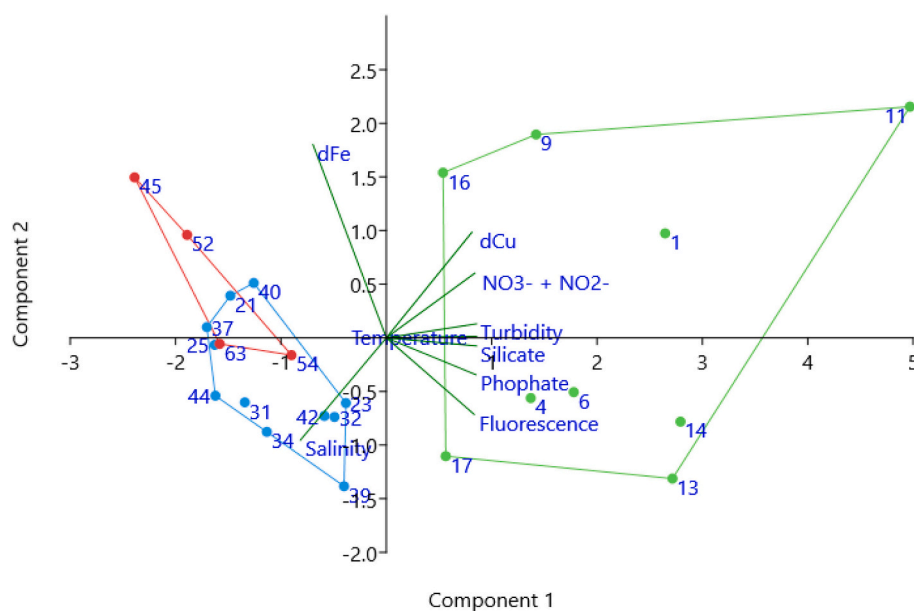
3. Results

3.1. Hydrographic characterization

Hydrographic, oxygen and pH data for each station are depicted in Table 1, and the description of the hydrographic conditions was recently reported by Mehlmann et al. (2020). The Macaronesia region presented a south to north sea surface temperature (SST) gradient (Fig. 1 from satellite image). The maximum SST was measured at the Cape Verde stations with average values of 22.33 ± 0.47 °C and minimum SST in Madeira (18.60 ± 0.18 °C). Around the Canary Islands, the mean SST was 19.18 ± 0.39 °C.

Sea surface salinity (SSS) values (Table 1) at Cape Verde were the lowest throughout the studied area, with values between 35.93 and 36.52. In the Canary Islands and Madeira the SSS were practically constant with mean values of 36.80 ± 0.06 and 36.72 ± 0.04, respectively. A gradient in dissolved oxygen concentration was also measured (Table 1), with concentrations around 214.5 ± 4.7 μmol kg^{-1} in the Cape Verde region, values of 228.3 ± 2.1 μmol kg^{-1} in the Canary Islands and 230.6 ± 1.0 μmol kg^{-1} around Madeira. The average pH at the studied stations was 8.07 ± 0.02 with the lowest values in the Cape Verde islands (8.05) and the highest (8.09) around the Madeira archipelago.

The fluorescence (not calibrated) decreases from south to north and it was given in an arbitrary unit (a.u.) approximately equal to mg m^{-3} of chlorophyll. Higher average concentrations were recorded in the Cape Verde archipelago (0.58 ± 0.31 a.u.), intermediate values in the Canary Islands (0.33 ± 0.19 a.u.) and lower amounts in the Madeira archipelago (0.15 ± 0.10 a.u.). At Cape Verde, stations 13 and 14 presented maximum fluorescence concentrations at 20 m depth (1.07 and 0.85 a.u., respectively) while the lowest value was observed at St. 17 (0.13 a.u.). In the Canaries, maximum values were recorded at St. 39 (0.65 a.u.) and 32 (0.56 a.u.) and the minimum at St. 37 (0.07 a.u.). Finally, in the Madeira archipelago the highest, fluorescence was observed at St. 54 (0.29 a.u.) and the lowest at St. 63 (0.09 a.u.).

The turbidity (Table 1) along the region ranged between 0.01 and 0.34 NTU. At Cape Verde, maximum values were recorded at St. 13 and 14 (mean value 0.28 ± 0.08 NTU) while all other stations presented a mean value of 0.03 ± 0.001 NTU. In the Canary Islands, maximum values of turbidity were found at St. 39, 40 and 42 (mean value = 0.043 ± 0.01 NTU) the other station presented lower values, around 0.02 ± 0.01 NTU. Finally, the Madeira region showed turbidity around 0.02 ± 0.01 NTU.

Fig. 3. Results of PCA analysis realized considering temperature, salinity, fluorescence, turbidity, dissolved Fe (dFe), dissolved Cu (dCu) and nutrients (nitrate and nitrate, phosphate and silicates) for the Macaronesia region. Green dots represent Cape Verde stations, blue dots Canary Island stations and with red colour Madeira samples.

Table 1

Location, temperature (°C), salinity, pH (total scale), dissolved oxygen concentration (μmol kg^{-1}) and fluorescence (a.u.) for each station measured at 20 m depth. Also included are nutrient concentrations (nitrites and nitrates, phosphates and silicates measured in μmol l^{-1}) obtained at around 20 m depth.

	Station	Latitude (°N)	Longitude (°E)	Temperature (°C)	Salinity	pH	O_2 (μmol kg^{-1})	Fluorescence (a.u.)	$NO_3^- + NO_2^-$ (μmol l^{-1})	PO_4^{3-} (μmol l^{-1})	$Si(OH)_4$ (μmol l^{-1})	Turbidity (NTU)
	1	16.9107	−25.1662	22.54	36.47	7.98	215.04	0.40	0.02	0.13	0.91	0.04
	4	16.5556	−24.3860	22.37	36.36	8.05	210.90	0.65	0.13	0.09	0.28	0.03
	6	14.8430	−24.2627	22.59	36.20	8.06	211.86	0.49	0.80	0.13	0.58	0.03
	9	14.8913	−23.5069	22.53	36.08	8.04	208.75	0.23	1.35	0.15	0.83	0.02
Cape Verde	11	15.1332	−23.2371	23.15	35.93	8.07	210.43	0.25	4.48	0.37	1.64	0.03
	13	16.1407	−22.9727	21.70	36.25	8.06	219.42	1.07	0.34	0.16	0.17	0.22
	14	16.6154	−22.9557	21.61	36.35	8.06	217.65	0.85	0.45	0.19	0.23	0.34
	16	16.8915	−24.8518	22.21	36.50	8.07	213.67	0.57	0.27	0.13	0.09	0.03
	17	17.5811	−24.2831	22.25	36.52	8.06	222.98	0.14	0.12	0.19	0.30	0.03
	21	27.6439	−17.9579	19.46	36.89	8.07	225.45	0.22	0.15	0.06	0.03	–
	23	27.9591	−17.6529	19.48	36.85	8.07	225.30	0.65	0.38	0.16	0.07	0.02
	25	28.0375	−17.3157	19.71	36.89	8.07	225.64	0.21	0.03	0.05	0.10	0.01
	31	28.0279	−16.7275	19.92	36.87	8.07	228.27	0.28	–	–	–	0.03
	32	28.0085	−16.6023	19.06	36.79	8.07	228.25	0.56	0.07	0.13	0.40	0.03
Canary Islands	34	28.3165	−16.3394	18.90	36.76	8.07	229.38	0.30	0.01	0.08	0.11	0.02
	37	28.3200	−15.9779	18.95	36.78	–	229.17	0.06	0.10	0.08	0.03	–
	39	27.8105	−15.8317	18.86	36.75	8.09	231.03	0.65	0.04	0.07	0.27	0.04
	40	27.6872	−15.7041	18.97	36.76	8.06	227.43	0.27	0.15	0.07	0.36	0.04
	42	27.9610	−15.3309	18.70	36.72	8.08	230.27	0.23	–	–	–	0.05
	44	29.1669	−15.5004	19.01	36.79	8.08	230.83	0.22	0.02	0.06	0.13	0.02
	45	30.0175	−16.0790	18.75	36.77	8.08	231.37	0.11	0.02	0.02	0.12	0.01
	52	32.4041	−16.5272	18.54	36.69	8.09	229.03	0.02	0.23	0.06	0.27	0.01
Madeira	54	32.6471	−16.5905	18.37	36.67	8.09	230.91	0.29	0.19	0.06	0.19	–
	63	32.6514	−17.1136	18.73	36.74	8.07	230.94	0.09	0.21	0.05	0.19	0.03

3.2. Iron speciation

The dFe speciation is shown in Table 2. The dFe concentration ranged from 0.46 to 1.32 nM (mean value 0.80 ± 0.25 nM) for all the regions (Fig. 4). Only four stations (St. 1, 13, 14 and 31) showed saturated ligand titrations, and the dFe speciation was not computed within the detection windows used in the investigation. At Cape Verde, the mean dFe concentration was 0.72 ± 0.28 nM and the maximum values were recorded at stations 9, 11 and 16 (1.08 ± 0.12 nM). The other stations showed lower concentrations (0.54 ± 0.08 nM). In the case of the Canary Islands, the mean dFe concentration was 0.80 ± 0.16 nM.

The minimum concentration was found at St. 39 (0.57 ± 0.03 nM) and the maximum at St. 40 (1.06 ± 0.10 nM). At Madeira, St. 63 (0.70 ± 0.28 nM) showed a dFe concentration similar to St. 54 (0.73 ± 0.13 nM), located between Madeira and Desertas Islands. At Desertas (St. 45) and Salvages Islands (St. 52) the dFe concentrations were similar (1.28 ± 0.06 nM). Considering that the Madeira archipelago comprises the islands of Salvages, Desertas and Madeira, the mean dFe for the area was 1.00 ± 0.33 nM. The oceanic stations (St. 17 CVOO, St. 44 ESTOC) presented different dFe concentrations, being lower in CVOO (St. 17, dFe = 0.46 ± 0.29 nM) than in ESTOC (St. 44, dFe = 0.71 ± 0.07 nM).

The L_{Fe} concentrations in the whole studied area (Fig. 4 and Table 2)

Table 2

Dissolved Fe concentrations (dFe, nM) and dFe speciation for all the studied stations. Labile Fe (Fe′, in pM), free inorganic Fe (pFe^{3+}) expressed as $-\log[Fe^{3+}]$ in M, Fe-binding ligands (L_{Fe}, in nM), excess of ligands (eL_{Fe}, in nM calculated as the difference between L_{Fe} and dFe), organically bound Fe (FeL, in nM), percentage of the metal organically complexed (%FeL), stability constant referred to Fe^{3+} ($\log K^{cond}_{Fe^{3+}L}$) and the reactivity of the metal-binding ligands in respect to the Fe^{3+} ($\log f_{Fe^{3+}L}$). "nd" means that the natural ligands were saturated in dFe.

	Station	dFe(nM)	Fe′ (pM)	pFe^{3+}	L_{Fe} (nM)	eL_{Fe} (nM)	FeL (nM)	%FeL	$\log K^{cond}_{Fe^{3+}L}$	$\log f_{Fe^{3+}L}$
Cape Verde	1	0.60 ± 0.10	nd	nd	nd	nd	nd	nd	nd	nd
	4	0.51 ± 0.19	2.28 ± 0.07	21.64 ± 23.17	1.47 ± 0.05	0.96	0.51	99.55	21.36 ± 0.01	12.53
	6	0.49 ± 0.04	1.14 ± 0.16	21.94 ± 22.79	1.81 ± 0.08	1.32	0.49	99.77	21.87 ± 0.46	13.13
	9	1.10 ± 0.17	11.7 ± 1.28	20.93 ± 21.89	1.66 ± 0.26	0.56	1.09	98.94	21.21 ± 0.19	12.43
	11	0.95 ± 0.08	14.3 ± 9.38	20.84 ± 21.03	1.10 ± 0.32	0.15	0.94	98.49	21.60 ± 0.34	12.64
	13	0.51 ± 0.06	nd	nd	nd	nd	nd	nd	nd	nd
	14	0.67 ± 0.06	nd	nd	nd	nd	nd	nd	nd	nd
	16	1.19 ± 0.12	3.25 ± 0.41	21.49 ± 22.39	1.78 ± 0.28	0.59	1.19	99.73	21.79 ± 0.21	13.04
	17	0.46 ± 0.29	9.56 ± 0.33	21.02 ± 22.48	0.52 ± 0.11	0.06	0.45	97.92	21.85 ± 0.38	12.56
	21	0.97 ± 0.27	31.9 ± 8.86	20.50 ± 21.05	1.01 ± 0.21	0.04	0.94	96.71	21.59 ± 0.23	12.59
	23	0.89 ± 0.12	8.68 ± 0.70	21.06 ± 22.16	1.17 ± 0.13	0.28	0.88	99.02	21.54 ± 0.11	12.61
	25	0.89 ± 0.03	7.47 ± 0.20	21.13 ± 22.70	1.34 ± 0.36	0.45	0.88	99.16	21.41 ± 0.26	12.54
	31	0.73 ± 0.04	nd	nd	nd	nd	nd	nd	nd	nd
Canary Islands	32	0.83 ± 0.19	5.67 ± 1.30	21.25 ± 21.89	1.28 ± 0.29	0.45	0.82	99.32	21.51 ± 0.32	12.62
	34	0.63 ± 0.02	5.18 ± 0.41	21.29 ± 22.39	1.56 ± 0.29	0.93	0.63	99.18	21.11 ± 0.17	12.31
	37	0.87 ± 0.04	11.5 ± 7.58	20.94 ± 21.12	1.30 ± 0.52	0.43	0.86	98.68	21.23 ± 0.37	12.34
	39	0.57 ± 0.03	5.73 ± 1.32	21.24 ± 21.88	0.94 ± 0.26	0.37	0.56	98.99	21.41 ± 0.29	12.39
	40	1.06 ± 0.10	25.50 ± 7.27	20.59 ± 21.14	1.36 ± 0.37	0.30	1.03	97.59	21.09 ± 0.22	12.23
	42	0.61 ± 0.07	10.00 ± 1.79	21.00 ± 21.75	1.61 ± 0.58	1.00	0.60	98.36	20.77 ± 0.27	11.98
	44	0.71 ± 0.07	6.02 ± 0.58	21.22 ± 22.23	1.22 ± 0.19	0.51	0.70	99.15	21.36 ± 0.20	12.44
	45	1.24 ± 0.30	14.4 ± 10.30	20.84 ± 20.99	1.33 ± 0.28	0.09	1.23	98.84	21.90 ± 0.48	13.03
Madeira	52	1.32 ± 0.18	15.70 ± 5.26	20.80 ± 21.28	1.47 ± 0.19	0.15	1.30	98.81	21.70 ± 0.46	12.87
	54	0.73 ± 0.13	28.60 ± 11.80	20.54 ± 20.93	0.84 ± 0.33	0.11	0.70	96.08	21.24 ± 0.37	12.16
	63	0.70 ± 0.28	5.62 ± 2.90	21.25 ± 21.54	1.10 ± 0.38	0.40	0.69	99.20	21.49 ± 0.35	12.53

showed an average concentration of 1.29 ± 0.32 nM. In the Cape Verde Islands (mean $L_{Fe} = 1.39 ± 0.50$ nM) the lowest concentration was found at the oceanic station (St. 17, 0.52 ± 0.11 nM) and the maximum at St. 6 (1.81 ± 0.08 nM). In the Canary Islands, the mean L_{Fe} concentration was 1.28 ± 0.21 nM with a maximum at St. 42 ($L_{Fe} = 1.61 ± 0.58$ nM) and minimum at St. 39 ($L_{Fe} = 0.94 ± 0.26$ nM). In the Madeira archipelago, the mean L_{Fe} concentration was 1.19 ± 0.27 nM. At St. 63, L_{Fe} presented a concentration of 1.10 ± 0.38 nM, while the maximum was observed at St. 52 and 45 (1.40 ± 0.10 nM). The L_{Fe} at the oceanic stations showed a concentration of 0.52 ± 0.11 nM at CVOO (St. 17), which increased to 1.22 ± 0.19 nM at ESTOC (St. 44).

Throughout the studied region, $\log K^{cond}_{Fe3+L}$ (Table 2) varied between 20.77 and 21.90 (mean value 21.45 ± 0.29). The different archipelagos showed similar mean $\log K^{cond}_{Fe3+L}$, and the oceanic stations presented values that fell within the range of the coastal stations. Based on the two ligands classification, all the samples corresponded to an L_2 ligand type with $\log K^{cond}_{Fe3+L} < 22$.

The Fe′, Fe^{3+}, FeL and eL_{Fe} parameters were estimated based on the dFe and L_{Fe} concentration. The average Fe′ concentration showed lower concentrations in Cape Verde (7.04 ± 5.52 pM), intermediate concentrations in the Canary Islands (11.77 ± 9.28 pM) and higher amounts in the Madeira archipelago (19.08 ± 9.47 pM). More than 98% of Fe′ was organically complexed (Table 2), with the lowest percentages at St. 21 (south of El Hierro) and St. 54 (between Madeira and Desertas) at ~96.4%. The mean FeL concentration for the entire studied region was 0.82 ± 0.25 nM with values oscillating between 0.45 nM and 1.30 nM. The mean FeL was 0.78 ± 0.33 nM in Cape Verde, 0.79 ± 0.16 nM in the Canary Islands and 0.98 ± 0.33 nM in the Madeira archipelago.

The solubility of Fe(III) oxy-hydroxide, was estimated taking into account the in situ values of pH, temperature and salinity (Liu and Millero, 1999). This is the predominant Fe(III) species at pH 8 and presented an overall mean concentration of 0.018 ± 0.001 nM. The solubility product of Fe(OH)$_3$, $\log K^*_{Fe(OH)3}$, took values between 3.9 and 4.2 while the hydrolysis constant for the same species, $\log \beta^*_3$, ranged from −14.7 to −14.9.

3.3. dCu speciation

The dCu speciation data are shown in Table 3 and Fig. 4. Natural ligands were saturated in dCu for stations 1, 4 and 16. As observed for Fe, Cu parameters also showed variations between and within the regions. Throughout the studied area, dCu ranged between 0.07 nM and 4.03 nM (mean concentration 0.91 ± 0.77 nM). Cape Verde presented the greatest variability of dCu with concentrations between 0.36 and 4.03 nM (mean concentration 1.30 ± 1.15 nM). Stations 1, 4 and 16 showed the highest dCu concentrations (4.03 ± 0.20 nM, 1.51 ± 0.20 nM and 1.98 ± 0.08 nM, respectively) within this area. The stations were close to one another and located towards the northwest of Cape Verde. Minimum dCu concentrations (~0.45 ± 0.09 nM) were recorded at the northeast stations (St. 13, 14 and 17). In the Canary archipelago, the average dCu concentration was 0.65 ± 0.15 nM and the maximum was found at St. 21 (1.05 ± 0.11 nM), while the rest of the stations showed similar concentrations (0.61 ± 0.08 nM). In the case of Madeira, St. 63 showed a dCu concentration similar to St. 54 (0.98 ± 0.03 nM and 0.93 ± 0.10 nM, respectively). The lowest concentration was observed in the Desertas Islands (St. 52, dCu = 0.07 ± 0.02 nM) and the highest in the Salvages Islands (St. 45, dCu = 1.09 ± 0.17 nM). The mean concentration observed in the Madeira archipelago was 0.77 ± 0.47 nM. As indicated for Fe, station 45 presented dCu concentrations similar to the Madeira stations than to the Canaries. dCu concentrations at the oceanic stations slightly increased from south to north, with 0.44 ± 0.07 nM at St. 17 and 0.57 ± 0.01 nM at St. 44.

The L_{Cu} (Table 3 and Fig. 4) for the entire studied region presented an average concentration of 1.05 ± 0.46 nM with values between 0.54 nM and 2.59 nM. At Cape Verde, the mean concentration was 1.29 ± 0.74 nM and the maximum (St. 14, 2.59 ± 0.91 nM) and minimum (St. 13, 0.62 ± 0.21 nM) were located at two nearby stations. In the Canary Islands, the mean L_{Cu} concentration was 0.86 ± 0.23 nM, the highest value was measured at St. 21 (1.31 ± 0.25 nM) and the lowest at St. 37 (0.54 ± 0.07 nM). In Madeira, St. 63 (1.32 ± 0.07 nM) presented a concentration higher than the one reported at St. 54 (1.18 ± 0.29 nM) and south to Desertas Islands (St. 52, 0.90 ± 0.14 nM), but similar to St. 45 (1.33 ± 0.19 nM). The mean L_{Cu} within the Madeira archipelago was 1.18 ± 0.20 nM. Regarding the oceanic stations (mean $L_{Cu} = 0.87 ±$
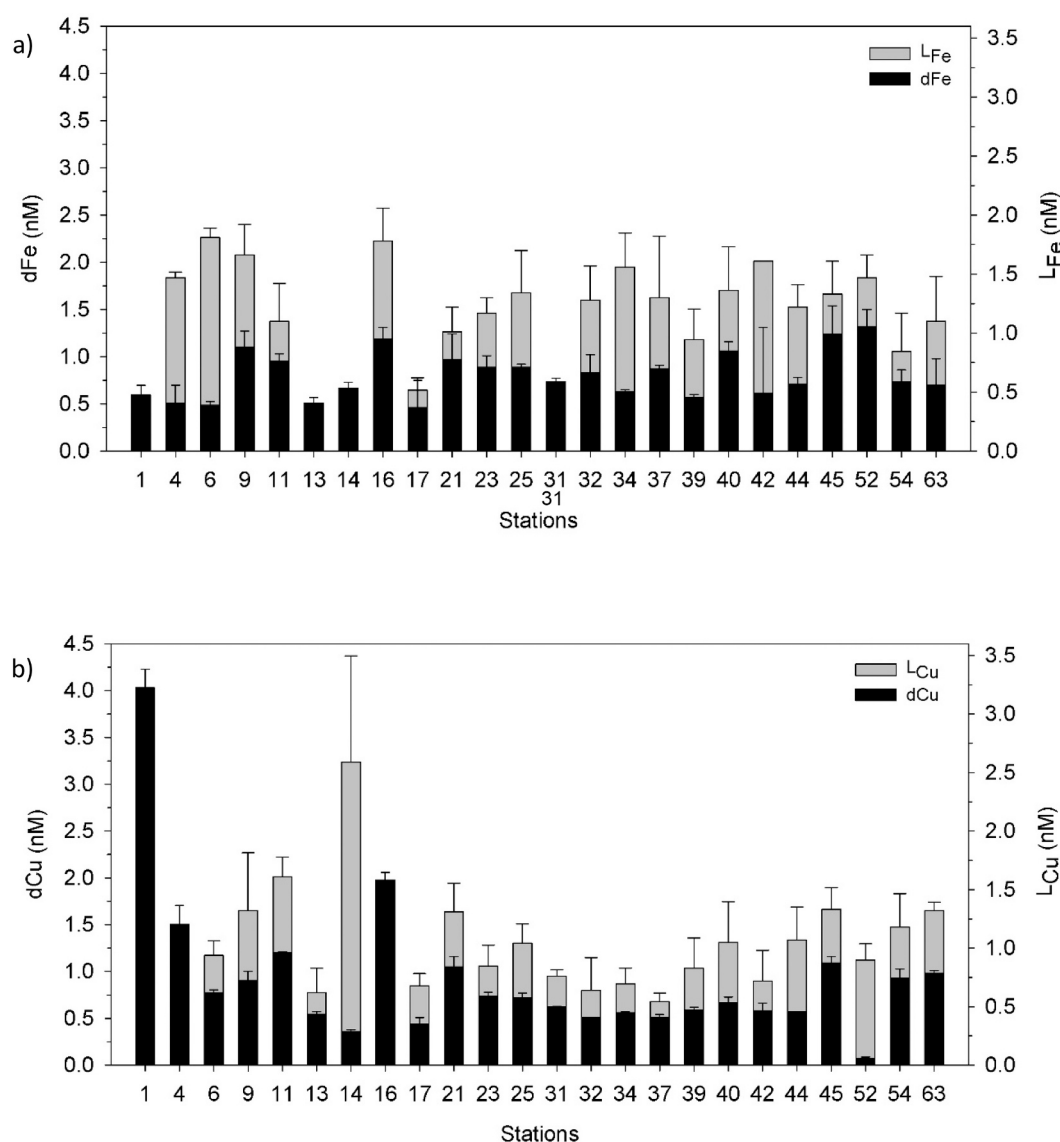
Fig. 4. a) Concentration of dissolved Fe (dFe, nM) and Fe-binding ligands (L$_{Fe}$, nM). b) Concentration of dissolved Cu (dCu, nM) and Fe-binding ligands (L$_{Cu}$, nM). Stations from 1 to 17 were in the Cape Verde region, from 21 to 44 in the Canary Islands, and from 45 to 63 in Madeira.

0.28 nM), St. 17 presented a lower concentration (0.68 ± 0.11 nM) than St. 44 (1.07 ± 0.28 nM).

In the Macaronesian region, log K$^{cond}_{Cu2+L}$ varied between 13.40 and 14.42 (mean value 13.92 ± 0.33) (Table 3). In Cape Verde, the mean log K$^{cond}_{Cu2+L}$ was 13.85 ± 0.41. Around the Canaries, the average value was 13.89 ± 0.30 with maximum at St. 37 (14.40 ± 0.13). In the Madeira archipelago, log K$^{cond}_{Cu2+L}$ showed a mean value of 14.10 ± 0.28. As regards the oceanic stations, St. 17 presented a higher log K$^{cond}_{Cu2+L}$ (14.22 ± 0.16) than St. 44 (13.54 ± 0.20). All stations showed log K$^{cond}_{Cu2+L}$ values higher than 13, corresponding to L$_1$-type ligands.

The Cu′ concentrations ranged between 0.14 and 5.70 pM (average of 1.59 ± 1.40 pM). The mean Cu′ concentration observed in Cape Verde (1.77 ± 2.11 pM) was similar to that obtained in the Canary Islands (1.73 ± 1.20 pM), and both of them were higher than the observed in the Madeira archipelago (0.93 ± 0.43 pM). The Cu^{2+} concentration ranged between 0.004 pM and 0.18 pM with an average value of 0.05 ± 0.04 pM.

The CuL concentrations (mean global value 0.74 ± 0.38 nM) indicated that more than 99% of Cu′ was complexed (an exception was St. 52 at 97.7%). In Cape Verde, CuL ranged between 0.36 and 1.20 nM (average 0.88 ± 0.56 nM). In the Canary region (average 0.60 ± 0.08 nM), the maximum was found at St. 21 (1.05 nM), the minimum at St. 32 and 37 (0.51 nM). Except for St. 52 (0.07 nM), the values recorded in Madeira (average 1.00 ± 0.08 nM) presented CuL concentrations higher than Cape Verde and the Canary Islands. The oceanic stations presented concentrations of 0.44 nM (St. 17) and 0.57 nM (St. 44).

The PCA analysis was conducted including all the stations. In the analysis (Fig. 3), the stations were considered as bulk data as well as clustered by archipelagos with similarities between Canary Island and Madeira samples. The PC1 explained 92.9% of the variance. Samples were split into stations that presented higher nutrient availability (NO$_3^-$ + NO$_2^-$, Si(OH)$_4$ and PO$_4^{3-}$, Table 1), dCu, temperature, turbidity and fluorescence on positive scores, that correspond with Cape Verde samples. Salinity and dFe concentration had negative scores and contain the Canary Islands and Madeira samples. Then PC1 mostly reflects the south to north gradient observed with a transition from more nutrient-rich to oligotrophic waters. This could indicate that the source of dFe is different from that of dCu and the rest of the nutrients.

The PC2 explained 7.1% of the variance, the strongest positive coefficients were related with dFe and dCu while the negatives with salinity and fluorescence. This distribution could be associated with a

Table 3

Dissolved Cu concentrations (nM) and dCu speciation for all the studied stations. Labile Cu (Cu', in pM), free inorganic Cu (Cu^{2+}, in pM), Cu-binding ligands (L_{Cu}, in nM), excess of ligands (Excess of L_{Cu}, in nM calculated as the difference between L_{Cu} and dCu), organically bound Cu (CuL, in nM), percentage of the metal organically complexed (%CuL), conditional stability constant for Cu^{2+} (log K^{cond}_{Cu2+L}), the reactivity of the metal-binding ligands in respect to Cu^{2+} (log f_{Cu2+L}). "nd" means that the natural ligands were saturated in dCu.

	Station	dCu (nM)	Cu(pM)	Cu^{2+} (pM)	L_{Cu} (nM)	eL_{Cu} (nM)	CuL (nM)	%CuL	log K^{cond}_{Cu2+L}	log f_{Cu2+L}
	1	4.03 ± 0.20	nd	nd	nd	nd	nd	nd	nd	nd
	4	1.51 ± 0.20	nd	nd	nd	nd	nd	nd	nd	nd
	6	0.78 ± 0.03	5.70 ± 0.75	0.18 ± 0.02	0.94 ± 0.12	0.16	0.77	99.27	13.40 ± 0.08	4.37
	9	0.90 ± 0.10	2.29 ± 0.40	0.07 ± 0.01	1.32 ± 0.49	0.42	0.90	99.75	13.48 ± 0.30	4.60
Cape Verde	11	1.20 ± 0.01	0.45 ± 0.04	0.01 ± 0.001	1.61 ± 0.17	0.40	1.20	99.96	14.33 ± 0.12	5.54
	13	0.54 ± 0.03	1.71 ± 0.52	0.05 ± 0.02	0.62 ± 0.21	0.08	0.54	99.68	14.09 ± 0.39	4.88
	14	0.36 ± 0.02	0.14 ± 0.02	0.004 ± 0.001	2.59 ± 0.91	2.24	0.36	99.96	13.58 ± 0.31	4.99
	16	1.98 ± 0.08	nd	nd	nd	nd	nd	nd	nd	nd
	17	0.44 ± 0.07	0.32 ± 0.04	0.01 ± 0.001	0.68 ± 0.11	0.24	0.44	99.93	14.22 ± 0.16	5.05
	21	1.05 ± 0.11	1.38 ± 0.14	0.04 ± 0.004	1.31 ± 0.25	0.26	1.05	99.87	13.97 ± 0.21	5.08
	23	0.74 ± 0.04	1.77 ± 0.31	0.06 ± 0.01	0.85 ± 0.18	0.11	0.74	99.76	14.08 ± 0.33	5.01
	25	0.72 ± 0.05	0.44 ± 0.06	0.01 ± 0.001	1.04 ± 0.17	0.32	0.72	99.94	14.21 ± 0.18	5.23
	31	0.63 ± 0.003	1.77 ± 0.25	0.06 ± 0.01	0.76 ± 0.05	0.14	0.62	99.72	13.91 ± 0.16	4.79
	32	0.51 ± 0.01	1.45 ± 0.06	0.05 ± 0.002	0.64 ± 0.28	0.13	0.51	99.71	13.91 ± 0.35	4.72
Canary Islands	34	0.56 ± 0.01	1.43 ± 0.71	0.04 ± 0.02	0.70 ± 0.14	0.14	0.56	99.74	13.96 ± 0.17	4.80
	37	0.51 ± 0.03	1.86 ± 0.17	0.06 ± 0.01	0.54 ± 0.07	0.03	0.51	99.64	14.40 ± 0.13	5.14
	39	0.59 ± 0.03	1.32 ± 0.15	0.04 ± 0.005	0.83 ± 0.26	0.24	0.59	99.78	13.77 ± 0.31	4.69
	40	0.67 ± 0.06	1.40 ± 0.09	0.04 ± 0.003	1.05 ± 0.35	0.38	0.67	99.79	13.60 ± 0.31	4.62
	42	0.58 ± 0.08	5.14 ± 0.53	0.16 ± 0.02	0.72 ± 0.26	0.14	0.58	99.12	13.40 ± 0.27	4.25
	44	0.57 ± 0002	1.03 ± 1.61	0.03 ± 0.05	1.07 ± 0.28	0.50	0.57	99.82	13.54 ± 0.20	4.57
	45	1.09 ± 0.07	0.55 ± 0.17	0.02 ± 0.01	1.33 ± 0.19	0.24	1.09	99.95	14.42 ± 0.22	5.54
Madeira	52	0.07 ± 0.02	1.52 ± 0.20	0.05 ± 0.01	0.90 ± 0.14	0.83	0.07	97.72	13.78 ± 0.12	4.73
	54	0.93 ± 0.10	0.72 ± 0.17	0.02 ± 0.01	1.18 ± 0.29	0.25	0.93	99.92	14.21 ± 0.36	5.28
	63	0.98 ± 0.03	0.94 ± 0.10	0.03 ± 0.003	1.32 ± 0.07	0.34	0.98	99.90	13.99 ± 0.30	5.11

biological utilization of dFe and dCu but also may indicate a corelation between dCu and $NO_3^- + NO_2^-$ and turbidity.

Through this analysis, Cape Verde is the region with the greatest dispersion, where St. 1, 9, 11 and 16 were different from the rest of the stations. However, the Canary Islands and Madeira samples are more aggregated.

4. Discussion

4.1. Island environment and processes

The metal distributions around the islands are affected by complex hydrographic dynamics and processes such as horizontal advection, vertical mixing, regenerations from sinking particles and resuspension from shelf sediments (Blain et al., 2008). Furthermore, for the Canary Islands and Madeira, a strong mesoscale variability was observed due to the interaction between the prevailing winds and currents with the landmasses (Caldeira et al., 2002; Caldeira and Sangrà, 2012; Sangrà et al., 2005). Islands act as barriers with differences in flow current perturbation and wind share between east and west (Sangrà et al., 2009). As a consequence, the mixing process which takes place in these waters also differs.

As the presence of microorganisms is also relevant in terms of metal speciation, it is important to remark that the mesoscale variability generated in the vicinity of oceanic islands also influences the phytoplankton community. On the island of Gran Canaria, the effect of wind stress on biological production has previously been studied (Arístegui and Montero, 2005; Basterretxea et al., 2002). It was observed that in the flanks and downstream of the island an enhancement of biological production was associated with wind-induced water upwelling (divergent boundary) or downwelling (convergent boundary).

The studied region, archipelagic waters, is also particularly complex to describe due to the variety of chemical processes that could take place. Firstly, surface waters are subject to photoreduction reactions affecting both metals and organic compounds. The photochemical reaction can occur by direct light absorption followed by a charge transfer between ligand and metal or by the production of radical species. As a result, the amount of metals in the solution could increase, the ligands

may decompose or the binding sites could be modified or lost, resulting in a ligand binding strength decrease (Barbeau, 2006; Moffett and Zika, 1987). These processes can enhance the bioavailability and reactivity of metals and may occur in solution or on the particle surface. In fact, the presence of suspended particulate matter decreases the concentration of surface metals due to the scavenging process. In the open ocean surface waters, the presence of particles is related to biological sources or dust deposition. In coastal areas, the particles could also be related to runoff, ravines inputs and suspended sediments, as well as anthropogenic sources. Other molecular aggregates may undergo scavenging. Within the dissolved fraction, the colloidal phase may contain both metal species and ligands. The formation of larger colloidal aggregates may increase the transport of metals to deeper layers and decrease their bioavailability (Wu et al., 2001). In addition, in coastal areas, human activities such as sewage discharge, power and desalination plants and industries could alter the chemistry of coastal water.

All these processes result in a very complex and heterogeneous set of compounds that constitute the ligand pool present in the seawater. Different assumptions have to be taken into account to apply the CLE-ACSV technique and obtain information about the bulk ligand concentration and characterization (Gerringa et al., 2014, 2021). In addition, pH, temperature, salinity and the chosen competitive ligand are key parameters. For this reason, the term "conditional" is used to indicate the stability constants determined by voltammetry under the selected experimental conditions.

4.2. dFe speciation

The surface concentrations of dFe measured along the Macaronesian coastal region (mean dFe = 0.80 ± 0.25 nM) were comparable with the results obtained in the whole Atlantic Ocean with values between 0.13 and 1.80 nM (Buck et al., 2015; Gledhill and van den Berg, 1994; Hatta et al., 2015; Rijkenberg et al., 2012). The oceanic stations (St. 17 and 44) showed dFe concentrations similar to those reported by other studies in the same region (Boye et al., 2006; Buck et al., 2015). In Cape Verde, the highest concentrations were observed at St. 9 and 11, the southeasternmost samples of the region, along with higher concentrations of $NO_3^- + NO_2^-$ and $Si(OH)_4$. For these stations, Mehlmann et al. (2020)

reported a wind speed (25.5 m s^{-1}) higher than the one observed in other locations (~9.8 m s^{-1}). Windy conditions can enhance the vertical diffusive mixing and supply dFe to the surface water from waters below (Rijkenberg et al., 2012) and from the sediment (Gerringa et al., 2008) as well as from the island due to the proximity of the coast. These resuspended sediments can favour the sequestration of dFe to deep waters via scavenging or be a source of Fe^{2+} if the particles undergo photoreduction processes in surface waters (Wells and Mayer, 1991). Two studies with transects from the oceanic region to the African coastal margin reported a trend with increasing dFe concentrations towards the coast (Hatta et al., 2015; Rijkenberg et al., 2012). In the study at hand, there were no evidences of contributions of dFe from the African dust, and the observed variations were associated with local processes.

The measured L$_{Fe}$ concentrations (0.52–1.81 nM) were in good agreement with the literature for the Atlantic Ocean (Boye et al., 2006, 2003; Buck et al., 2015; Gerringa et al., 2006; Gledhill and van den Berg, 1994; Rijkenberg et al., 2008; Thuróczy et al., 2010). Most of these investigations showed a variation of L$_{Fe}$ between 0.8 and 2 nM and different ligand sources were suggested (biological production, organic matter remineralization, benthic fluxes and dust deposition). No clear relationship was observed between the L$_{Fe}$ and the fluorescence peaks detected during the cruise, where stations with high L$_{Fe}$ concentrations did not correspond with high fluorescence. Minimum L$_{Fe}$ at St.17 was

associated with oceanic waters. For coastal stations, a relationship was observed between wind conditions, biological activity and water depth with the concentration of L$_{Fe}$. The effect of the wind on the water mixing and the resuspension of dFe and L$_{Fe}$ can be important at the shallower stations and could be coupled with a biological enhancement. Stations 1, 13 and 14 presented shallow depths (63 m, 35 m and 31 m, respectively), and had the highest turbidity and saturated titration curves, which could be associated with resuspension of L$_{Fe}$ from bottom sediments. Station 6 presented high L$_{Fe}$, low dFe concentrations, windy conditions, high fluorescence and high concentrations of NO$_3^-$ + NO$_2^-$ and Si(OH)$_4$. At this location, both turbulence (induced by wind) and biological activity may control the ligand and metal concentrations. The east coasts of Tenerife and Gran Canaria (St. 34 and 42) were characterized by windy conditions, high L$_{Fe}$, low dFe but low fluorescence concentrations. These locations (St. 34 and 42) were close to urbanized areas where the anthropogenic ligand sources (sewage discharge, desalination plants and industries) along with the water mixing induced by the wind could explain the L$_{Fe}$ and dFe values. Station 39, situated in the southwest part of Gran Canaria, showed low L$_{Fe}$, low dFe and high concentrations of fluorescence and Si(OH)$_4$. Arístegui et al. (1997) reported an enhancement of primary production on the west coast of Gran Canaria, associated with both wind stirring and local water upwelling, which could explain the decrease of dFe due to biological uptake. On the
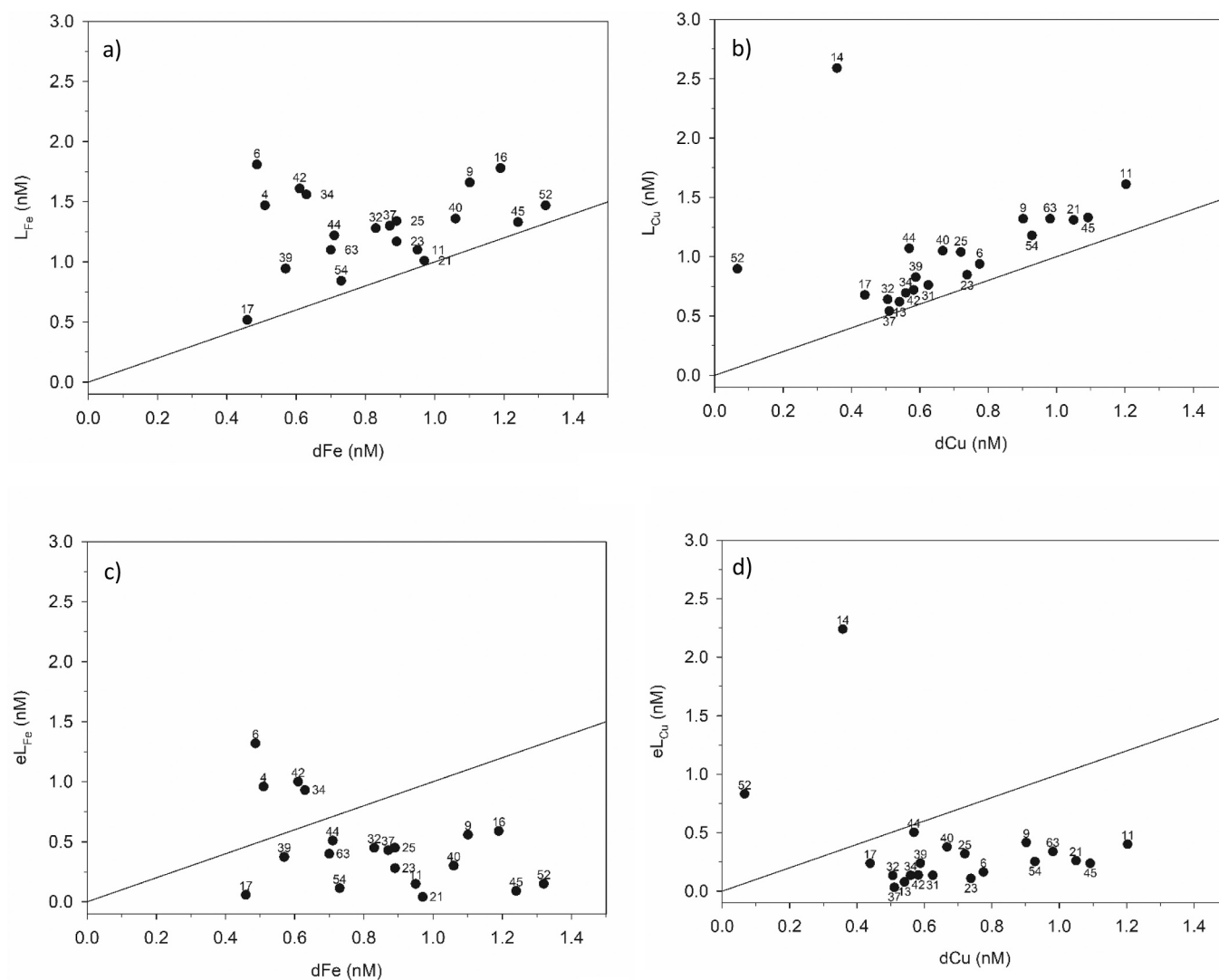
Fig. 5. Correlation between ligand and dissolved metal concentrations for Fe (a) and Cu (b). Relationship between excess ligand and dissolved metal concentration for Fe (c) and Cu (d). The solid line represents a 1:1 relationship.

other hand, at St. 25, 31 and 32, as reported for the coast of Gran Canaria (Arístegui et al., 1997; Arístegui and Montero, 2005; Basterretxea et al., 2002), convergent or divergent fronts could be present along either side of the wake region and produce water sinking or upwelling, respectively, which could influence the metal and ligand distribution.

The dFe and L_{Fe} concentrations were linearly correlated (Fig. 5). The ratio L_{Fe}/dFe indicates the saturation state of ligands and, whether precipitation is favoured or not (Thuróczy et al., 2011). This behaviour highlights the role of ligands in stabilizing dFe in surface water. All stations (except stations 1, 13, 14 and 31 that presented saturated titration curves) showed a ratio higher than 1 as reported for coastal areas and marginal seas (Kondo et al., 2007; Mellett and Buck, 2020) and could be related with a similar origin of dFe and L_{Fe}. Higher ratios were observed at stations 4, 6, 34 and 42, where L_{Fe} concentrations were greater than dFe (eL_{Fe} values were close to or greater than 1 nM). Stations 4 (L_{Fe}/dFe = 2.88) and 6 (L_{Fe}/dFe = 3.72) presented relatively high fluorescence values (0.65 and 0.49 a.u., respectively), which could indicate a biological production of ligands. Thuróczy et al. (2011) reported a ratio of around 4.4 for surface waters with high phytoplankton activity. Stations 34 (L_{Fe}/dFe = 2.48) and 42 (L_{Fe}/dFe = 2.64) ratios were related to water mixing induced by the wind. Fig. 5 shows how these stations differ from the other samples.

The log K^{cond}_{Fe3+L} obtained in this work (21.45 ± 0.29) was in the range of values (18.8–22.85) reported in the literature for oceanic waters in this region (Boye et al., 2006, 2003; Buck et al., 2015; Gerringa et al., 2006; Gledhill and van den Berg, 1994; Rijkenberg et al., 2008; Thuróczy et al., 2010). As detected in the Macaronesia region, only one ligand type was normally measured in the Northeast Atlantic region (Boye et al., 2006, 2003; Gerringa et al., 2006; Rijkenberg et al., 2008; Thuróczy et al., 2010), L_1 or L_2. Buck et al. (2015) reported data for a second ligand class, probably associated with the use of a larger detection window (25 µM SA). Our samples presented log K^{cond}_{Fe3+L} values lower than 22 (L_2-type) in agreement with the literature on the region (Gerringa et al., 2007; Thuróczy et al., 2010). On the other hand, the lower value reported at St. 42 matched with the results reported by Boye et al. (2006, 2003). Voltammetry results do not provide information about the nature of the compounds detected, but they do allow us to compare the conditional constants obtained with those of compounds already identified through incubation experiments or processes. Siderophores have been detected in surface water with log K^{cond}_{Fe3+L} values between 21 and 24 (Bundy et al., 2018; Witter et al., 2000) in regions with atmospheric dust deposition. Humic Substances have also been detected with strong ligand constants (Laglera et al., 2011; Laglera and van den Berg, 2009). The presence of weaker ligands (logK^{cond}_{Fe3+L} < 22) has been related to the grazing of phytoplankton by zooplankton and with the bacterial remineralization of organic sinking particles (Poorvin et al., 2011; Sato et al., 2007). In addition, Witter et al. (2000), González et al. (2019) and Arreguin et al. (2021) also reported the complexing capacity of individual ligands in seawater (i.e. catechin, sinapic acid, gallic acid, gentisic acid, apoferritin, alterobactin, desferrioxamine, enterobactin and ferrichrome) in a wide range, from L_1 to L_2-type ligands.

The variability observed for Fe′ (range between 1.14 and 31.90 pM) was slightly higher than that described for the surface oceanic waters of the Northeast Atlantic Ocean (Boye et al., 2006, 2003; Gledhill and van den Berg, 1994), where concentration between 1.4 and 26.9 pM were obtained. The Fe′ concentration gradient with the lowest values at Cape Verde and highest at Madeira follow the trend observed in the excess ligand concentration. Most of the FeL concentrations (0.45–1.30 nM) were similar to the values indicated for the oceanic region (Boye et al., 2006, 2003; Gledhill and van den Berg, 1994), which presented concentrations between 0.54 and 1.77 nM.

The obtained theoretical concentration of Fe(OH)$_3$ (0.018 ± 0.001 nM) was higher than the observed concentration of Fe^{3+} (between 10^{-21} and 10^{-22} M). The precipitation of hydroxides was not favoured due to the low concentration of Fe^{3+}. It has been demonstrated that the

presence of organic binding ligands increases the solubility of Fe (i.e. Kuma et al., 1996; Liu and Millero, 1999).

The average log $f_{Fe}^{3+}{}_L$ obtained along the Macaronesia region (12.62 ± 0.43, Table 2) agreed with the results reported for the Northeast Atlantic surface waters (Buck et al., 2015; Gerringa et al., 2017; Thuróczy et al., 2010), with values between 12 and 13.7. Higher log $f_{Fe}^{3+}{}_L$ values indicate a higher capacity of the ligand to bind dFe.

4.3. dCu speciation

The measured dCu surface concentration in the Macaronesia region (mean value 0.91 ± 0.77 nM) was comparable with the results reported for the Atlantic Ocean (Jacquot and Moffett, 2015; Kramer, 1986; Kremling, 1985; Roshan and Wu, 2015; Saager et al., 1997). The maximum measured dCu concentration, at St. 1 (4.03 ± 0.20 nM), was in the range of the values reported by Buckley and van den Berg (1986) for the surface water in the same region (3.6–5.9 nM). The Cape Verde stations presented the highest dCu variability. The highest concentrations were found around the northwestern islands (St. 1, 4 and 16), corresponding with a relatively high surface fluorescence (>0.40 a.u.). Furthermore, the northeastern stations (St. 1, 4 and 16) should be the ones most affected by the currents arriving from the Canary Islands, and by the mixing processes which occur in the Cape Verde Frontal Zone (Pelegrí et al., 2017; Peña-Izquierdo et al., 2012) but could also be accentuated by the strong winds near St. 1 (Mehlmann et al., 2020). Jacquot and Moffett (2015) suggested that the sediments and shelf can be a source of dCu for the region between Cape Verde and Mauritania. However, the shallowest stations (St. 13 and 14) presented the lowest dCu concentration along with the oceanic station (St. 17). The chemical properties of the sediment determine the effect on the surrounding waters, but also the biological activities can change the amounts of dCu and L_{Cu} present in surface waters. The small increase in concentration registered between the Canary Islands (dCu = 0.65 ± 0.15 nM) and Madeira (dCu = 0.77 ± 0.47 nM) was reflected in the results of Jacquot and Moffett (2015) and Roshan and Wu (2015).

The correlation between dCu and salinity (Fig. 6) observed in the Macaronesia region was compared with the results reported in the western North Atlantic Ocean for oceanic waters (Jacquot and Moffett, 2015; Roshan and Wu, 2015). The Madeira data were observed to be within the range described by these authors; Cape Verde values (excluding stations 1, 4 and 16) followed a different trend, while the
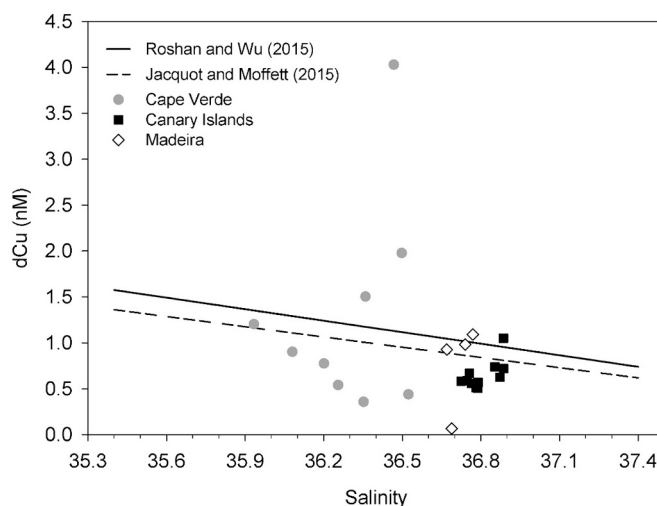

Fig. 6. Dissolved Cu (dCu, nM) vs. salinity for Cape Verde region (grey circles), Canary Islands (black squares) and Madeira (empty rhombuses). Stations 1, 4 and 16 were not included. The correlation reported by Roshan and Wu (2015) was dCu = − 2.35 S + 39.1 (R^2 = 0.97) while the trend described by Jacquot and Moffett (2015) was dCu = − 0.37 S + 14.6 (R^2 = 0.80).

Canary Islands data presented a different distribution. Roshan and Wu (2015) associated the linearity between the parameters with a long residence time of dCu in the surface mixed layer. Deviations observed in our data could be related to the processes that differentiate coastal from oceanic waters described above, where St. 1, 4 and 16 are the most affected by the mixing of the waters in the Cape Verde Frontal Zone.

The L_{Cu} concentrations recorded throughout the Macaronesia archipelagos (mean L_{Cu} = 1.05 ± 0.46 nM) were lower than the ones obtained by Jacquot and Moffett (2015) for the oceanic area, whose results between Mauritania and Portugal (~35 m depth) presented values between 2 and 3.69 nM. As indicated for L_{Fe}, at St. 13 and 14, the biological activity could explain the lowest (St.13, 0.62 ± 0.21 nM) and highest (St.14, 2.59 ± 0.91 nM) L_{Cu} concentrations observed in the Cape Verde region. Both stations presented low dCu concentrations and the highest fluorescence and turbidity value. Furthermore, these locations were shallow and the contribution of L_{Cu} from the bottom sediments should also be considered. Low L_{Cu}, dCu and fluorescence values observed at CVOO (St. 17) and in open waters between Tenerife and Gran Canaria (St. 37) supports the hypothesis that coastal waters represent a source of dCu and Cu-ligands for the nearby areas by biological activity and/or by the contribution from the sediments and the coast. As suggested for L_{Fe}, windy conditions can increase the water mixing and favour the resuspension from benthic sediments (Jacquot and Moffett, 2015) and explain the high L_{Cu} concentrations reported at St. 9 (1.32 ± 0.49 nM), 11 (1.61 ± 0.17 nM) and 21 (1.31 ± 0.24 nM). Stations 9 and 11 also presented high concentrations of $NO_3^- + NO_2^-$ and $Si(OH)_4$ which could also imply an input of nutrients and ligands from deeper waters associated with mixing processes.

Based on these results, a linear multiple regression was applied to determine which environmental variables were related to the concentration of ligands in seawater. For L_{Fe} no significant (*p*-value>0.05) correlations were observed. However, L_{Cu} concentration was correlated with water turbidity, $NO_3^- + NO_2^-$ concentration and fluorescence, following the equation below:

$$L_{Cu} = 1.173 + 0.147 \cdot [NO_3^- + NO_2^-] + 6.104 \cdot \text{Turbidity} - 1.292 \cdot \text{Fluorescence}$$
(14)

The determination coefficient (R^2) of the linear model presented a value of 0.7, with a standard error or estimation of 0.3 nM and the variability of L_{Cu} associated with the parameters is significant (p-value <0.05).

The linear model explains almost 70% of the variability observed in the coastal waters of the Macaronesia islands. Within this fit, the role of turbidity outweighs the effect of fluorescence and $NO_3^- + NO_2^-$ concentration. Turbidity is an important factor that differentiates coastal from oceanic regions, as the distance from the coast decreases, this variable can increase due to both terrigenous input and bottom sediment mobilisation. Fluorescence can be related to primary production, which is generally higher in coastal regions than in oceanic waters. On the other hand, the presence of $NO_3^- + NO_2^-$ could be related to higher productivity, anthropogenic sources and, consequently, organic ligands. Among the variety of substances that form dissolved organic matter are amino acids, which can react and bind to dissolved metals (Benner, 2011; Devez et al., 2015).

The concentration of L_{Cu} and dCu were positively correlated (Fig. 5). The ratio L_{Cu}/dCu, representing the saturation state of the ligands with Cu, was always higher than 1. On the other hand, the relation between eL_{Cu} and dCu concentrations indicates that at St. 14 and 52 the concentrations of ligands were much higher than at the other stations. The biological production (St. 14) and the water mixing with resuspension from the sediment (St. 52) could increase L_{Cu} concentrations.

The log K^{cond}_{Cu2+L} obtained in this study (13.92 ± 0.33) corresponds with L_1-type ligands (log K^{cond}_{Cu2+L} > 13). The results were comparable with data reported by other authors in the same region (Jacquot and Moffett, 2015; log K^{cond}_{Cu2+L} = 13.57 ± 0.48). Coastal stations

presented log K^{cond}_{Cu2+L} values between 13.40 and 14.42, higher than the ones observed in the nearshore waters of the West Florida Shelf (Mellett and Buck, 2020), whose values range between 13.09 and 13.31 and where riverine inputs of ligands were detected. Inshore waters of the Bermudas (Oldham et al., 2014) presented two ligand classes (log K^{cond}_{Cu2+L1} = 14–15.1 and log K^{cond}_{Cu2+L2} = 12.6–14.1), and the environment was affected by different anthropogenic activities. For offshore waters, Mellett and Buck (2020) also reported a single ligand type (log K^{cond}_{Cu2+L} = 13.85–13.91) with values more similar to those obtained in the Macaronesia region for both coastal and oceanic waters. In offshore surface waters near the Bermudas (Oldham et al., 2014) two ligand classes were detected with log K^{cond}_{Cu2+L1} = 15.1–14 and log K^{cond}_{Cu2+L2} = 13.7–12.6. Also, in the continental slope of the northeast Pacific, Whitby et al. (2018) observed two ligand types in oceanic (log K^{cond}_{Cu2+L1} = 15.5 and log K^{cond}_{Cu2+L2} = 12.9) and nearshore stations (log K^{cond}_{Cu2+L1} = 15.5 and log K^{cond}_{Cu2+L2} = 12.6). For the Sargasso Sea, Moffett et al. (1990) suggest that strong ligands are related to a recent biological origin rather than to refractory humic substances.

The amounts of Cu´ and Cu^{2+} (1.59 ± 1.40 pM and 0.05 ± 0.04 pM, the respective mean concentrations) were very low compared to the dCu concentrations (0.91 ± 0.76 nM). Free Cu can be toxic and inhibit the growth of phytoplankton. The toxicity depends on each organism, but it is estimated that at concentrations higher than 10 pM, some phytoplankton and cyanobacteria species reduce the growth rate (Brand et al., 1986; Coale and Bruland, 1990; Sunda and Lewis, 1978). However, if the free Cu concentration is too low (below 0.01 pM), it is insufficient to allow the acquisition of Fe by marine organisms (Maldonado et al., 2006; Peers et al., 2005). The Cu^{2+} concentrations observed in the Macaronesia region did not exceed the toxicity values but could limit the growth of phytoplankton due to Cu^{2+} deficiency, as reported for oceanic waters (Jacquot and Moffett, 2015; Moffett and Dupont, 2007). Most of the dCu concentrations were observed as CuL, with more than 99% of dCu bound with ligands, as reported in the literature (Buck and Bruland, 2005; Coale and Bruland, 1990; Moffett and Dupont, 2007; Whitby et al., 2018).

Throughout the Macaronesia region, log f_{Cu2+L} ranges between 4.25 and 5.54 (average value 4.90 ± 0.34). Higher values indicate a higher capacity of the ligand to bind dCu. While the average value was lower than the one observed in nearshore waters of the West Florida Shelf (5.15–5.10) described by Mellett and Buck (2020), the range observed in the Macaronesia region was wider. The West Florida offshore waters presented values more similar to those obtained at St.17 (log f_{Cu2+L} = 5.05).

When comparing the speciation results of Fe with those of Cu, it was observed that the maximums and minimums of dFe and dCu or L_{Fe} and L_{Cu} were not measured at the same stations. The sources of metals and ligands were not always the same between stations, as well as the processes which removed them from surface water, especially in coastal waters where several processes are taking place at the same time. For example, the chemical properties of the sediments, the organisms which form the phytoplankton community or the dynamic process, are not the same in the region. However, at many stations (10 over 24), the ranges of concentrations of L_{Fe} and L_{Cu} were similar. Buck et al. (2015) and Jacquot and Moffett (2015) suggested for the North Atlantic Ocean that the ligands could have a similar source or at least a part of L_{Fe} was not specific for Fe. The same was also suggested for the West Florida Shelf waters (Mellett and Buck, 2020). At the stations where the biological activity and the wind stress were not important, other factors could explain the presence of high values of dissolved metal and ligands. The horizontal advection, the isopycnal mixing and the dissolution from lithogenic particles (Blain et al., 2008) are processes which alter the speciation of metals in coastal waters but their effects cannot be demonstrated with the available data.

5. Conclusion

The knowledge about the iron and copper speciation in the coastal waters is quite important to be able to understand the global biogeochemical cycles of Fe and Cu. Among the Atlantic Ocean, the surrounding waters of Macaronesia islands are relevant to the role of the Atlantic circulation. They are close to the upwelling and within the subtropical gyre. Regarding Fe speciation, dFe was found in excess of L_{Fe} concentrations, and a complexation percentage higher than 98% was observed. Only one ligand (concentrations ranging between 0.56 and 2.96 nM) was detected with log K^{cond}_{Fe3+L} values lower than 22 (L_2-type). On the other hand, strong Cu-complexing ligands dominate dCu speciation. More than 99% of dCu was complexed by strong ligands (L_1-type) of log $K^{cond}_{Cu2+L} = 13.92 \pm 0.33$ and only one complex was detected at concentrations varying between 0.54 and 2.59 nM. As a consequence of the high complexation, the concentration of Cu^{2+} (0.004–0.18 pM) was below the toxicity limit but could inhibit the growth of certain phytoplankton species. This distribution of dFe and dCu seems to be related to the hydrographic parameters (temperature, salinity, turbidity, fluorescence and nutrient concentration), while the content of L_{Cu} was mostly related to the turbidity, fluorescence and $NO_3^- + NO_2^-$ concentrations that were fitted to a multilinear regression equation.

Throughout the study region, dFe and dCu presented different distributions of extreme values. However, the concentration ranges of L_{Fe} and L_{Cu} overlapped at many stations even if the maximums and minimums were obtained at different locations.

The chemistry of Fe and Cu is also dependent on the wind-mediated mixing processes and fluorescence. A relationship was observed between the maximum and minimum values obtained and the presence of strong winds and high fluorescence, both for dFe and dCu concentrations, as well as for L_{Fe} and L_{Cu} concentrations. Differences between coastal and oceanic concentrations of dissolved metals and ligands were observed in the regions of the Canary Islands and Cape Verde.

According to the current investigation, the coastal stations present a higher concentration of dissolved metals and ligands than the oceanic stations. Therefore, coastal waters of the Macaronesia region could be a source of metals and ligands, possibly associated with the resuspension of sediments by the action of currents and wind and the biological activity. The data reported in this study improve our knowledge about the Fe and Cu biogeochemical cycles in coastal waters.

Declaration of Competing Interest

The authors declare that they have no known competing financial interests or personal relationships that could have appeared to influence the work reported in this paper.

Acknowledgments

References

Abualhaija, M.M., Whitby, H., van den Berg, C.M.G., 2015. Competition between copper and iron for humic ligands in estuarine waters. Mar. Chem. 172, 46–56. https://doi.org/10.1016/j.marchem.2015.03.010.

Annett, A.L., Lapi, S., Ruth, T.J., Maldonado, M.T., 2008. The effects of Cu and Fe availability on the growth and Cu:C ratios of marine diatoms. Limnol. Oceanogr. 53, 2451–2461. https://doi.org/10.4319/lo.2008.53.6.2451.

Arístegui, J., Montero, M.F., 2005. Temporal and spatial changes in plankton respiration and biomass in the Canary Islands region: the effect of mesoscale variability. J. Mar. Syst. 54, 65–82. https://doi.org/10.1016/j.jmarsys.2004.07.004.

Arístegui, J., Tett, P., Hernández-Guerra, A., Basterretxea, G., Montero, M.F., Wild, K., Sangrá, P., Hernández-Leon, S., Canton, M., García-Braun, J.A., Pacheco, M., Barton, E.D., 1997. The influence of island-generated eddies on chlorophyll distribution: a study of mesoscale variation around Gran Canaria. Deep Sea Res. Part I Oceanogr. Res. Pap. 44, 71–96. https://doi.org/10.1016/S0967-0637(96)00093-3.

Arreguin, M.L., González, A.G., Pérez-Almeida, N., Arnone, V., González-Dávila, M., Santana-Casiano, J.M., 2021. The role of gentisic acid on the Fe(III) redox chemistry in marine environments. Mar. Chem. 234, 104003 https://doi.org/10.1016/j.marchem.2021.104003.

Baker, A.R., Jickells, T.D., Witt, M., Linge, K.L., 2006. Trends in the solubility of iron, aluminium, manganese and phosphorus in aerosol collected over the Atlantic Ocean. Mar. Chem. 98, 43–58. https://doi.org/10.1016/j.marchem.2005.06.004.

Barbeau, K., 2006. Photochemistry of organic iron(III) complexing ligands in oceanic systems. Photochem. Photobiol. 82 (6), 1505–1516. https://doi.org/10.1111/j.1751-1097.2006.tb09806.x.

Basterretxea, G., Barton, E.D., Tett, P., Sangrá, P., Navarro-Perez, E., Arístegui, J., 2002. Eddy and deep chlorophyl maximum response to wind-shear in the lee of Gran Canaria. Deep Sea Res. Part I Oceanogr. Res. Pap. 49, 1087–1101. https://doi.org/10.1016/S0967-0637(02)00009-2.

Benner, R., 2011. Loose ligands and available iron in the ocean. Proc. Natl. Acad. Sci. 108, 893–894. https://doi.org/10.1073/pnas.1018163108.

Blain, S., Tréguer, P., Belviso, S., Bucciarelli, E., Denis, M., Desabre, S., Fiala, M., Martin Jézéquel, V., Le Fèvre, J., Mayzaud, P., Marty, J.-C., Razouls, S., 2001. A biogeochemical study of the island mass effect in the context of the iron hypothesis: Kerguelen Islands, Southern Ocean. Deep Sea Res. Part I Oceanogr. Res. Pap. 48, 163–187. https://doi.org/10.1016/S0967-0637(00)00047-9.

Blain, S., Quéguiner, B., Armand, L., Belviso, S., Bombled, B., Bopp, L., Bowie, A., Brunet, C., Brussaard, C., Carlotti, F., Christaki, U., Corbière, A., Durand, I., Ebersbach, F., Fuda, J.-L., Garcia, N., Gerringa, L., Griffiths, B., Guigue, C., Guillerm, C., Jacquet, S., Jeandel, C., Laan, P., Lefèvre, D., Lo Monaco, C., Malits, A., Mosseri, J., Obernosterer, I., Park, Y.-H., Picheral, M., Pondaven, P., Remenyi, T., Sandroni, V., Sarthou, G., Savoye, N., Scouarnec, L., Souhaut, M., Thuiller, D., Timmermans, K., Trull, T., Uitz, J., van Beek, P., Veldhuis, M., Vincent, D., Viollier, E., Vong, L., Wagener, T., 2007. Effect of natural iron fertilization on carbon sequestration in the Southern Ocean. Nature 446, 1070–1074. https://doi.org/10.1038/nature05700.

Blain, S., Sarthou, G., Laan, P., 2008. Distribution of dissolved iron during the natural iron-fertilization experiment KEOPS (Kerguelen Plateau, Southern Ocean). Deep Sea Res. Part II Top. Stud. Oceanogr. 55, 594–605. https://doi.org/10.1016/j.dsr2.2007.12.028.

Bowie, A.R., van der Merwe, P., Quéroué, F., Trull, T., Fourquez, M., Planchon, F., Sarthou, G., Chever, F., Townsend, A.T., Obernosterer, I., Sallée, J.-B., Blain, S., 2015. Iron budgets for three distinct biogeochemical sites around the Kerguelen Archipelago (Southern Ocean) during the natural fertilisation study, KEOPS-2. Biogeosciences 12, 4421–4445. https://doi.org/10.5194/bg-12-4421-2015.

Boye, M., Aldrich, A.P., Van Berg, C.M.G., Den, J., De, J.T.M., Veldhuis, M., De Baar, H.J. W., 2003. Horizontal gradient of the chemical speciation of iron in surface waters of the northeast Atlantic Ocean. Mar. Chem. 80, 129–143.

Boye, M., Aldrich, A., Van Berg, C.M.G., Den, J., De, J.T.M., Nirmaier, H., Veldhuis, M., Timmermans, K.R., De Baar, H.J.W., 2006. The chemical speciation of iron in the north-east Atlantic Ocean. Deep. Res. I 53, 667–683. https://doi.org/10.1016/j.dsr.2005.12.015.

Brand, L.E., Sunda, W.G., Guillard, R.R.L., 1986. Reduction of marine phytoplankton reproduction rates by copper and cadmium. J. Exp. Mar. Bio. Ecol. 96, 225–250. https://doi.org/10.1016/0022-0981(86)90205-4.

Bruland, K.W., Rue, E.L., Donat, J.R., Skrabal, S.A., Moffett, J.W., 2000. Intercomparison of voltammetric techniques to determine the chemical speciation of dissolved copper in a coastal seawater sample. Anal. Chim. Acta 405, 99–113. https://doi.org/10.1016/S0003-2670(99)00675-3.

Buck, K.N., Bruland, K.W., 2005. Copper speciation in San Francisco Bay: a novel approach using multiple analytical windows. Mar. Chem. 96, 185–198. https://doi.org/10.1016/j.marchem.2005.01.001.

Buck, K.N., Lohan, M.C., Berger, C.J.M., Bruland, K.W., 2007. Dissolved iron speciation in two distinct river plumes and an estuary: implications for riverine iron supply. Limnol. Oceanogr. 52, 843–855. https://doi.org/10.4319/lo.2007.52.2.0843.

Buck, K.N., Selph, K.E., Barbeau, K.A., 2010. Iron-binding ligand production and copper speciation in an incubation experiment of Antarctic Peninsula shelf waters from the Bransfield Strait, Southern Ocean. Mar. Chem. 122, 148–159. https://doi.org/10.1016/j.marchem.2010.06.002.

Buck, K.N., Moffett, J., Barbeau, K.A., Bundy, R.M., Kondo, Y., Wu, J., 2012. The organic complexation of iron and copper: an intercomparison of competitive ligand

exchange-adsorptive cathodic stripping voltammetry (CLE-ACSV) techniques. Limnol. Oceanogr. Methods 10, 496–515. https://doi.org/10.4319/lom.2012.10.496.

Buck, K.N., Sohst, B., Sedwick, P.N., 2015. The organic complexation of dissolved iron along the U.S. GEOTRACES (GA03) North Atlantic section. Deep Res. Part II Top. Stud. Oceanogr. 116, 152–165. https://doi.org/10.1016/j.dsr2.2014.11.016.

Buckley, P.J.M., van den Berg, C.M.G., 1986. Copper complexation profiles in the Atlantic Ocean. Mar. Chem. 19, 281–296. https://doi.org/10.1016/0304-4203(86)90028-9.

Bundy, R.M., Barbeau, K.A., Buck, K.N., 2013. Sources of strong copper-binding ligands in Antarctic Peninsula surface waters. Deep Sea Res. Part II Top. Stud. Oceanogr. 90, 134–146. https://doi.org/10.1016/j.dsr2.2012.07.023.

Bundy, R.M., Boiteau, R.M., McLean, C., Turk-Kubo, K.A., McIlvin, M.R., Saito, M.A., Van Mooy, B.A.S., Repeta, D.J., 2018. Distinct siderophores contribute to Iron cycling in the mesopelagic at station ALOHA. Front. Mar. Sci. 5, 1–15. https://doi.org/10.3389/fmars.2018.00061.

Caldeira, R.M.A., Sangrà, P., 2012. Complex geophysical wake flows. Ocean Dyn. 62, 683–700. https://doi.org/10.1007/s10236-012-0528-6.

Caldeira, R.M.A., Groom, S., Miller, P., Pilgrim, D., Nezlin, N.P., 2002. Sea-surface signatures of the island mass effect phenomena around Madeira Island, Northeast Atlantic. Remote Sens. Environ. 80, 336–360. https://doi.org/10.1016/S0034-4257(01)00316-9.

Campos, M.L.A.M., van den Berg, C.M.G., 1994. Determination of copper complexation in sea water by cathodic stripping voltammetry and ligand competition with salicylaldoxime. Anal. Chim. Acta 284, 481–496.

Clayton, T.D., Byrne, R.H., 1993. Spectrophotometric seawater pH measurements: total hydrogen ion concentration scale calibration of m-cresol purple and at-sea results. Deep Sea Res. Part I Oceanogr. Res. Pap. 40, 2115–2129. https://doi.org/10.1016/0967-0637(93)90048-8.

Coale, K.H., Bruland, K.W., 1990. Spatial and temporal variability in copper complexation in the North Pacific. Deep Sea Res. Part A. Oceanogr. Res. Pap. 37, 317–336. https://doi.org/10.1016/0198-0149(90)90130-N.

Conway, T.M., John, S.G., 2014. Quantification of dissolved iron sources to the North Atlantic Ocean. Nature 511, 212–215. https://doi.org/10.1038/nature13482.

Croot, P.L., Johansson, M., 2000. Determination of iron speciation by cathodic stripping voltammetry in seawater using the competing ligand 2-(2-thiazolylazo)-p-cresol (TAC). Electroanalysis 12, 565–576. https://doi.org/10.1002/(SICI)1521-4109(200005)12:8<565::AID-ELAN565>3.0.CO;2-L.

Cutter, G., Andersson, P., Codispoti, L., Croot, P., Francois, R., Lohan, M., Obata, H., Rutgers van der Loeff, M., 2010. Sampling and Sample-handling Protocols for GEOTRACES Cruises.

Devez, A., Achterberg, E., Gledhill, M., 2015. 15 metal ion-binding properties of phytochelatins and related ligands. In: Metallothioneins and Related Chelators. De Gruyter, pp. 441–482.

Duce, R.a., Tindale, N.W., 1991. Atmospheric transport of iron and its deposition in the ocean. Limnol. Oceanogr. 36, 1715–1726. https://doi.org/10.4319/lo.1991.36.8.1715.

Elrod, V.A., Berelson, W.M., Coale, K.H., Johnson, K.S., 2004. The flux of iron from continental shelf sediments: a missing source for global budgets. Geophys. Res. Lett. 31 https://doi.org/10.1029/2004GL020216.

Garnier, C., Pižeta, I., Mounier, S., Benaïm, J.Y., Branica, M., 2004. Influence of the type of titration and of data treatment methods on metal complexing parameters determination of single and multi-ligand systems measured by stripping voltammetry. Anal. Chim. Acta 505, 263–275. https://doi.org/10.1016/j.aca.2003.10.066.

Gelado-Caballero, M.D., López-García, P., Prieto, S., Patey, M.D., Collado, C., Hérnández-Brito, J.J., 2012. Long-term aerosol measurements in Gran Canaria, Canary Islands: particle concentration, sources and elemental composition. J. Geophys. Res. Atmos. 117 https://doi.org/10.1029/2011JD016646.

Gerringa, L.J.A., Veldhuis, M.J.W., Timmermans, K.R., Sarthou, G., de Baar, H.J.W., 2006. Co-variance of dissolved Fe-binding ligands with phytoplankton characteristics in the Canary Basin. Mar. Chem. 102, 276–290. https://doi.org/10.1016/j.marchem.2006.05.004.

Gerringa, L.J.A., Rijkenberg, M.J.A., Wolterbeek, H.T., Verburg, T.G., Boye, M., de Baar, H.J.W., 2007. Kinetic study reveals weak Fe-binding ligand, which affects the solubility of Fe in the Scheldt estuary. Mar. Chem. 103, 30–45. https://doi.org/10.1016/j.marchem.2006.06.002.

Gerringa, L.J.A., Blain, S., Laan, P., Sarthou, G., Veldhuis, M.J.W., Brussaard, C.P.D., Viollier, E., Timmermans, K.R., 2008. Fe-binding dissolved organic ligands near the Kerguelen Archipelago in the Southern Ocean (Indian sector). Deep Sea Res. Part II Top. Stud. Oceanogr. 55, 606–621. https://doi.org/10.1016/j.dsr2.2007.12.007.

Gerringa J.A., L., Gledhill, M., Ardiningsih, I., Muntjewerf, N., Laglera M., L., 2021. Comparing CLE-AdCSV applications using SA and TAC to determine the Fe-binding characteristics of model ligands in seawater. Biogeosci. 18 (19), 5265–5289. https://doi.org/10.5194/bg-18-5265-2021.

Gerringa, L.J.A., Rijkenberg, M.J.A., Thuróczy, C.E., Maas, L.R.M., 2014. A critical look at the calculation of the binding characteristics and concentration of iron complexing ligands in seawater with suggested improvements. Environ. Chem. 11, 114–136. https://doi.org/10.1071/EN13072.

Gerringa, L.J.A., Slagter, H.A., Bown, J., van Haren, H., Laan, P., de Baar, H.J.W., Rijkenberg, M.J.A., 2017. Dissolved Fe and Fe-binding organic ligands in the Mediterranean Sea – GEOTRACES G04. Mar. Chem. 194, 100–113. https://doi.org/10.1016/j.marchem.2017.05.012.

Gledhill, M., Buck, K.N., 2012. The organic complexation of iron in the marine environment: a review. Front. Microbiol. 3, 1–17. https://doi.org/10.3389/fmicb.2012.00069.

Gledhill, M., Gerringa, L.J.A., 2017. The effect of metal concentration on the parameters derived from complexometric titrations of trace elements in seawater—a model study. Front. Mar. Sci. 4, 1–15. https://doi.org/10.3389/fmars.2017.00254.

Gledhill, M., van den Berg, C.M.G., 1994. Determination of complexation of iron(III) with natural organic complexing ligands in seawater using cathodic stripping voltammetry. Mar. Chem. 47, 41–54. https://doi.org/10.1016/0304-4203(94)90012-4.

Gledhill, M., Achterberg, E.P., Li, K., Mohamed, K.N., Rijkenberg, M.J.A., 2015. Influence of ocean acidification on the complexation of iron and copper by organic ligands in estuarine waters. Mar. Chem. 177, 421–433. https://doi.org/10.1016/j.marchem.2015.03.016.

González, A.G., Cadena-Aizaga, M.I., Sarthou, G., González-Dávila, M., Santana-Casiano, J.M., 2019. Iron complexation by phenolic ligands in seawater. Chem. Geol. 511, 380–388. https://doi.org/10.1016/j.chemgeo.2018.10.017.

González-Dávila, M., Santana-Casiano, J.M., Rueda, M.J., Llinás, O., González-Dávila, E.F., 2003. Seasonal and interannual variability of sea-surface carbon dioxide species at the European Station for Time Series in the Ocean at the Canary Islands (ESTOC) between 1996 and 2000. Glob. Biogeochem. Cycles 17. https://doi.org/10.1029/2002GB001993.

González-Dávila, M., Santana-Casiano, J.M., González, A.G., Pérez, N., Millero, F.J., 2009. Oxidation of copper(I) in seawater at nanomolar levels. Mar. Chem. 115, 118–124. https://doi.org/10.1016/j.marchem.2009.07.004.

Gordon, R.M., Johnson, K.S., Coale, K.H., 1998. The behaviour of iron and other trace elements during the IronEx-I and PlumEx experiments in the Equatorial Pacific. Deep Sea Res. Part II Top. Stud. Oceanogr. 45, 995–1041. https://doi.org/10.1016/S0967-0645(98)00012-5.

Grasshoff, K., Kremling, K., Ehrhardt, M., 1999. Methods of seawater analysis. In: Methods of Seawater Analysis, Third. ed. Wiley, Germany. https://doi.org/10.1002/9783527613984.

Hatta, M., Measures, C.I., Wu, J., Roshan, S., Fitzsimmons, J.N., Sedwick, P., Morton, P., 2015. An overview of dissolved Fe and Mn distributions during the 2010–2011 U.S. GEOTRACES north Atlantic cruises: GEOTRACES GA03. Deep. Res. Part II 116, 117–129. https://doi.org/10.1016/j.dsr2.2014.07.005.

Heller, M.I., Croot, P.L., 2015. Copper speciation and distribution in the Atlantic sector of the Southern Ocean. Mar. Chem. 173, 253–268. https://doi.org/10.1016/j.marchem.2014.09.017.

Hudson, R.J.M., Covault, D.T., Morel, F.M.M., 1992. Investigations of iron coordination and redox reactions in seawater using 59Fe radiometry and ion-pair solvent extraction of amphiphilic iron complexes. Mar. Chem. 38, 209–235. https://doi.org/10.1016/0304-4203(92)90035-9.

Hutchins, D.A., Witter, A.E., Butler, A., Luther, G.W., 1999. Competition among marine phytoplankton for different chelated iron species. Nature 400, 858–861. https://doi.org/10.1038/23680.

Jacquot, J.E., Moffett, J.W., 2015. Copper distribution and speciation across the international GEOTRACES section GA03. Deep Sea Res. Part II Top. Stud. Oceanogr. 116, 187–207. https://doi.org/10.1016/j.dsr2.2014.11.013.

Kondo, Y., Takeda, S., Furuya, K., 2007. Distribution and speciation of dissolved iron in the Sulu Sea and its adjacent waters. Deep Sea Res. Part II Top. Stud. Oceanogr. 54, 60–80. https://doi.org/10.1016/j.dsr2.2006.08.019.

Kramer, C.J.M., 1986. Apparent copper complexation capacity and conditional stability constants in North Atlantic waters. Mar. Chem. 18, 335–349. https://doi.org/10.1016/0304-4203(86)90016-2.

Kremling, K., 1985. The distribution of cadmium, copper, nickel, manganese, and aluminium in surface waters of the open Atlantic and European shelf area. Deep Sea Res. Part A. Oceanogr. Res. Pap. 32, 531–555. https://doi.org/10.1016/0198-0149(85)90043-3.

Kuma, K., Nishioka, J., Matsunaga, K., 1996. Controls on iron(III) hydroxide solubility in seawater: the influence of pH and natural organic chelators. Limnol. Oceanogr. 41, 396–407. https://doi.org/10.4319/lo.1996.41.3.0396.

Laglera, L., Battaglia, G., van den Berg, C.M., 2011. Effect of humic substances on the iron speciation in natural waters by CLE/CSV. Mar. Chem. 127 (1–4), 134–143. https://doi.org/10.1016/j.marchem.2011.09.003.

Laglera M., L., van den Berg G., C.M., 2009. Evidence for geochemical control of iron by humic substances in seawater. Limnol. Oceanogr. 54 (2), 610–619. https://doi.org/10.4319/lo.2009.54.2.0610.

Liu, X., Millero, F.J., 1999. The solubility of iron hydroxide in sodium chloride solutions. Geochim. Cosmochim. Acta 63, 3487–3497. https://doi.org/10.1016/S0016-7037(99)00270-7.

Liu, X., Millero, F.J., 2002. The solubility of iron in seawater. Mar. Chem. 77, 43–54. https://doi.org/10.1016/S0304-4203(01)00074-3.

López-García, P., Gelado-Caballero, M.D., Patey, M.D., Hernández-Brito, J.J., 2021. Atmospheric fluxes of soluble nutrients and Fe: more than three years of wet and dry deposition measurements at Gran Canaria (Canary Islands). Atmos. Environ. 246, 118090 https://doi.org/10.1016/j.atmosenv.2020.118090.

Maldonado, M.T., Price, N.M., 1999. Utilization of iron bound to strong organic ligands by plankton communities in the subarctic Pacific Ocean. Deep. Res. Part II Top. Stud. Oceanogr. 46, 2447–2473.

Maldonado, M.T., Allen, A.E., Chong, J.S., Lin, K., Leus, D., Karpenko, N., Harris, S.L., 2006. Copper-dependent iron transport in coastal and oceanic diatoms. Limnol. Oceanogr. 51, 1729–1743. https://doi.org/10.4319/lo.2006.51.4.1729.

Mehlmann, M., Quack, B., Atlas, E., Hepach, H., Tegtmeier, S., 2020. Natural and anthropogenic sources of bromoform and dibromomethane in the oceanographic and biogeochemical regime of the subtropical North East Atlantic. Environ. Sci. Process. Impacts 22, 679–707. https://doi.org/10.1039/C9EM00599D.

Mellett, T., Buck, K.N., 2020. Spatial and temporal variability of trace metals (Fe, Cu, Mn, Zn, Co, Ni, Cd, Pb), iron and copper speciation, and electroactive Fe-binding

humic substances in surface waters of the eastern Gulf of Mexico. Mar. Chem. 227, 103891 https://doi.org/10.1016/j.marchem.2020.103891.

Mills, M.M., Ridame, C., Davey, M., La Roche, J., Geider, R.J., 2005. Erratum: iron and phosphorus co-limit nitrogen fixation in the eastern tropical North Atlantic (Nature (2004) 429 (292-294)). Nature 435, 232. https://doi.org/10.1038/nature03632.

Moffett, J.W., Zika, R.G., 1987. Solvent extraction of copper acetylacetonate in studies of copper (II) speciation in seawater. Marine Chemistry 21 (4), 301–313.

Moffett, J.W., Dupont, C., 2007. Cu complexation by organic ligands in the sub-arctic NW Pacific and Bering Sea. Deep. Res. I 54, 586–595. https://doi.org/10.1016/j.dsr.2006.12.013.

Moffett, J.W., Zika, R.G., Brand, L.E., 1990. Distribution and potential sources and sinks of copper chelators in the Sargasso Sea. Deep Sea Res.Part A. Oceanogr. Res. Pap. 37, 27–36. https://doi.org/10.1016/0198-0149(90)90027-S.

Monteiro, P.M.S., Orren, M.J., 1985. Trace metals in the Southern Ocean: on the geochemistry of copper. Mar. Chem. 15, 345–355. https://doi.org/10.1016/0304-4203(85)90045-3.

Moore, J.K., Doney, S.C., Glover, D.M., Fung, I.Y., 2001. Iron cycling and nutrient-limitation patterns in surface waters of the world ocean. Deep. Res. Part II Top. Stud. Oceanogr. 49, 463–507. https://doi.org/10.1016/S0967-0645(01)00109-6.

Morel, F.M.M., Price, N.M., 2003. The biogeochemical cycles of trace metals in the oceans. Science (80-.) 300, 944–947. https://doi.org/10.1126/science.1083545.

Morel, N.M.L., Rueter, J.C., Morel, F.M.M., 1978. Copper toxicity to Skeletonema costatum (Bacillariophyceae). J. Phycol. 14, 43–48. https://doi.org/10.1111/j.1529-8817.1978.tb00629.x.

Morel, F.M.M., Kustka, A.B., Shaked, Y., 2008. The role of unchelated Fe in the iron nutrition of phytoplankton. Limnol. Oceanogr. 53, 400–404. https://doi.org/10.4319/lo.2008.53.1.0400.

Oldham, V.E., Swenson, M.M., Buck, K.N., 2014. Spatial variability of total dissolved copper and copper speciation in the inshore waters of Bermuda. Mar. Pollut. Bull. 79, 314–320. https://doi.org/10.1016/j.marpolbul.2013.12.016.

Omanović, D., Garnier, C., Pižeta, I., 2015. ProMCC: an all-in-one tool for trace metal complexation studies. Mar. Chem. 173, 25–39. https://doi.org/10.1016/j.marchem.2014.10.011.

Peers, G., Quesnel, S.-A., Price, N.M., 2005. Copper requirements for iron acquisition and growth of coastal and oceanic diatoms. Limnol. Oceanogr. 50, 1149–1158. https://doi.org/10.4319/lo.2005.50.4.1149.

Pelegrí, J.L., Peña-Izquierdo, J., Machín, F., Meiners, C., Presas-Navarro, C., 2017. Oceanography of the Cape Verde Basin and Mauritanian slope waters. In: Ramos, A., Ramil, F., Sanz, J.L. (Eds.), Deep-Sea Ecosystems off Mauritania. Springer, Netherlands, Dordrecht, pp. 119–153. https://doi.org/10.1007/978-94-024-1023-5_3.

Peña-Izquierdo, J., Pelegrí, J.L., Pastor, M.V., Castellanos, P., Emelianov, M., Gasser, M., Salvador, J., Vázquez-Domínguez, E., 2012. The continental slope current system between Cape Verde and the Canary Islands. Sci. Mar. 76, 65–78. https://doi.org/10.3989/scimar.03607.18C.

Pižeta, I., Sander, S.G., Hudson, R.J.M., Omanović, D., Baars, O., Barbeau, K.A., Buck, K. N., Bundy, R.M., Carrasco, G., Croot, P.L., Garnier, C., Gerringa, L.J.A., Gledhill, M., Hirose, K., Kondo, Y., Laglera, L.M., Nuester, J., Rijkenberg, M.J.A., Takeda, S., Twining, B.S., Wells, M., 2015. Interpretation of complexometric titration data: an intercomparison of methods for estimating models of trace metal complexation by natural organic ligands. Mar. Chem. 173, 3–24. https://doi.org/10.1016/j.marchem.2015.03.006.

Planquette, H., Statham, P.J., Fones, G.R., Charette, M.A., Moore, C.M., Salter, I., Nédélec, F.H., Taylor, S.L., French, M., Baker, A.R., Mahowald, N., Jickells, T.D., 2007. Dissolved iron in the vicinity of the Crozet Islands, Southern Ocean. Deep Sea Res. Part II Top. Stud. Oceanogr. 54, 1999–2019. https://doi.org/10.1016/j.dsr2.2007.06.019.

Poorvin, L., Sander, S.G., Velasquez, I., Ibisanmi, E., LeCleir, G.R., Wilhelm, S.W., 2011. A comparison of Fe bioavailability and binding of a catecholate siderophore with virus-mediated lysates from the marine bacterium *Vibrio alginolyticus* PWH3a. J. Exp. Mar. Bio. Ecol. 399, 43–47. https://doi.org/10.1016/j.jembe.2011.01.016.

Raapoto, H., Martinez, E., Petrenko, A., Doglioli, A., Gorgues, T., Sauzède, R., Maamaatuaiahutapu, K., Maes, C., Menkes, C., Lefèvre, J., 2019. Role of iron in the Marquesas Island Mass Effect. J. Geophys. Res. Ocean. 124, 7781–7796. https://doi.org/10.1029/2019JC015275.

Raven, J.A., Evans, M.C.W., Korb, R.E., 1999. The role of trace metals in photosynthetic electron transport in O2-evolving organisms. Photosynth. Res. 60, 111–150. https://doi.org/10.1023/a:1006282714942.

Rico, M., López, A., Santana-Casiano, J.M., Gonzàlez, A.G., Gonzàlez-Dàvila, M., 2013. Variability of the phenolic profile in the diatom *Phaeodactylum tricornutum* growing under copper and iron stress. Limnol. Oceanogr. 58, 144–152. https://doi.org/10.4319/lo.2013.58.1.0144.

Rijkenberg, M.J.A., Powell, C.F., Dall'Osto, M., Nielsdottir, M.C., Patey, M.D., Hill, P.G., Baker, A.R., Jickells, T.D., Harrison, R.M., Achterberg, E.P., 2008. Changes in iron speciation following a Saharan dust event in the tropical North Atlantic Ocean. Mar. Chem. 110, 56–67. https://doi.org/10.1016/j.marchem.2008.02.006.

Rijkenberg, M.J.A., Steigenberger, S., Powell, C.F., Haren, H., Patey, M.D., Baker, A.R., Achterberg, E.P., 2012. Fluxes and distribution of dissolved iron in the eastern (sub-) tropical North Atlantic Ocean. Glob. Biogeochem. Cycles 26. https://doi.org/10.1029/2011GB004264.

Robinson, J., Popova, E.E., Srokosz, M.A., Yool, A., 2016. A tale of three islands: downstream natural iron fertilization in the Southern Ocean. J. Geophys. Res. Ocean. 121, 3350–3371. https://doi.org/10.1002/2015JC011319.

Roshan, S., Wu, J., 2015. The distribution of dissolved copper in the tropical-subtropical North Atlantic across the GEOTRACES GA03 transect. Mar. Chem. 176, 189–198. https://doi.org/10.1016/j.marchem.2015.09.006.

Ruacho, A., Bundy, R.M., Till, C.P., Roshan, S., Wu, J., Barbeau, K.A., 2020. Organic dissolved copper speciation across the U.S. GEOTRACES equatorial Pacific zonal transect GP16. Mar. Chem. 225 https://doi.org/10.1016/j.marchem.2020.103841.

Rue, E.L., Bruland, K.W., 1995. Complexation of iron(III) by natural organic ligands in the central North Pacific as determined by a new competitive ligand equilibration/adsorptive cathodic stripping voltammetric method. Mar. Chem. 50, 117–138. https://doi.org/10.1016/0304-4203(95)00031-L.

Saager, P.M., de Baar, H.J.W., de Jong, J.T.M., Nolting, R.F., Schijf, J., 1997. Hydrography and local sources of dissolved trace metals Mn, Ni, Cu, and Cd in the northeast Atlantic Ocean. Mar. Chem. 57, 195–216. https://doi.org/10.1016/S0304-4203(97)00038-8.

Sangrà, P., Pelegrí, J.L., Hernández-Guerra, A., Arregui, I., Martín, J.M., Marrero-Díaz, A., Martínez, A., Ratsimandresy, A.W., Rodríguez-Santana, A., 2005. Life history of an anticyclonic eddy. J. Geophys. Res. Ocean. 110, 1–19. https://doi.org/10.1029/2004JC002526.

Sangrà, P., Pascual, A., Rodríguez-Santana, Á., Machín, F., Mason, E., McWilliams, J.C., Pelegrí, J.L., Dong, C., Rubio, A., Arístegui, J., Marrero-Díaz, Á., Hernández-Guerra, A., Martínez-Marrero, A., Auladell, M., 2009. The canary Eddy corridor: a major pathway for long-lived eddies in the subtropical North Atlantic. Deep Sea Res. Part I Oceanogr. Res. Pap. 56, 2100–2114. https://doi.org/10.1016/j.dsr.2009.08.008.

Santana-Casiano, J.M., Quack, B., 2021. Metal (Iron and copper) complexation from water samples during POSEIDON cruise POS533 (AIMAC). PANGAEA. https://doi.org/10.1594/PANGAEA.933690.

Santana-Casiano, J.M., González-Dávila, M., Millero, F.J., 2005. Oxidation of nanomolar level of Fe(II) with oxygen in natural waters. Environ. Sci. Technol. 39, 2073–2079. https://doi.org/10.1021/es049748y.

Santana-Casiano, J.M., González-Dávila, M., González, A.G., Rico, M., López, A., Martel, A., 2014. Characterization of phenolic exudates from *Phaeodactylum tricornutum* and their effects on the chemistry of Fe(II)-Fe(III). Mar. Chem. 158, 10–16. https://doi.org/10.1016/j.marchem.2013.11.001.

Sato, M., Takeda, S., Furuya, K., 2007. Iron regeneration and organic iron(III)-binding ligand production during in situ zooplankton grazing experiment. Mar. Chem. 106, 471–488. https://doi.org/10.1016/j.marchem.2007.05.001.

Semeniuk, D.M., Cullen, J.T., Johnson, W.K., Gagnon, K., Ruth, T.J., Maldonado, M.T., 2009. Plankton copper requirements and uptake in the subarctic Northeast Pacific Ocean. Deep Sea Res. Part I Oceanogr. Res. Pap. 56, 1130–1142. https://doi.org/10.1016/j.dsr.2009.03.003.

Semeniuk, D.M., Bundy, R.M., Payne, C.D., Barbeau, K.A., Maldonado, M.T., 2015. Acquisition of organically complexed copper by marine phytoplankton and bacteria in the northeast subarctic Pacific Ocean. Mar. Chem. 173, 222–233. https://doi.org/10.1016/j.marchem.2015.01.005.

Sunda, W.G., 1989. Trace metal interactions with marine phytoplankton. Biol. Oceanogr. 6, 411–442.

Sunda, W.G., Lewis, J.A.M., 1978. Effect of complexation by natural organic ligands on the toxicity of copper to a unicellular alga, *Monochrysis lutheri*. Limnol. Oceanogr. 23, 870–876. https://doi.org/10.4319/lo.1978.23.5.0870.

Thuróczy, C.-E., Gerringa, L.J.A., Klunder, M.B., Middag, R., Laan, P., Timmermans, K.R., de Baar, H.J.W., 2010. Speciation of Fe in the Eastern North Atlantic Ocean. Deep Sea Res. Part I Oceanogr. Res. Pap. 57, 1444–1453. https://doi.org/10.1016/j.dsr.2010.08.004.

Thuróczy, C.E., Gerringa, L.J.A., Klunder, M.B., Laan, P., de Baar, H.J.W., 2011. Observation of consistent trends in the organic complexation of dissolved iron in the Atlantic sector of the Southern Ocean. Deep Res. Part II Top. Stud. Oceanogr. 58, 2695–2706. https://doi.org/10.1016/j.dsr2.2011.01.002.

Twining, B.S., Baines, S.B., 2013. The trace metal composition of marine phytoplankton. Annu. Rev. Mar. Sci. 5, 191–215. https://doi.org/10.1146/annurev-marine-121211-172322.

Wells L., W., Mayer M., L., 1991. Variations in the chemical lability of iron in estuarine, coastal and shelf waters and its implications for phytoplankton. Mar. Chem. 32 (2–4), 195–210. https://doi.org/10.1016/0304-4203(91)90038-X.

Whitby, H., Posacka, A.M., Maldonado, M.T., van den Berg, C.M.G., 2018. Copper-binding ligands in the NE Pacific. Mar. Chem. 204, 36–48. https://doi.org/10.1016/j.marchem.2018.05.008.

Witter, A.E., Hutchins, D.A., Butler, A., Luther, G.W., 2000. Determination of conditional stability constants and kinetic constants for strong model Fe-binding ligands in seawater. Mar. Chem. 69, 1–17. https://doi.org/10.1016/S0304-4203(99)00087-0.

Wolfe-Simon, F., Grzebyk, D., Schofield, O., Falkowski, P.G., 2005. The role and evolution of superoxide dismutases in algae. J. Phycol. 41, 453–465. https://doi.org/10.1111/j.1529-8817.2005.00086.x.

Wu, J., Boyle, E., Sunda, W., Wen, L.-S., 2001. Soluble and colloidal iron in the oligotrophic North Atlantic and North Pacific. Science (80-.) 293, 847–849. https://doi.org/10.1126/science.1059251.